GEORGIA INSTITUTE OF TECHNOLOGY
ENGINEERING EXPERIMENT STATION

PROJECT INITIATION

Date: November 3, 1975

Project Title: Low Energy Experiment to Measure a Weak Coupling of the Neutrino Current

Project No.: B-461

Project Director: T. P. Lang

Sponsor: National Science Foundation

Agreement Period: From 10/1/75   Until 12/31/76*

Type Agreement: Grant No. PHY75-21295

*9 month budget period plus 6 months
for submission of required reports,

Amount: $79,353 EES + $20,647 Physics (Sub-project G-41-642) = $100,000 Total

Reports Required: Annual Letter Technical; Final Report

Sponsor Contact Person:

Technical Matters
Dr. William S. Rodney
Director of Nuclear Physics
National Science Foundation
Washington, D. C. 20550

Administrative Matters
Thru OCA
Mr. Gaylord L. Ellis
Grants Officer
National Science Foundation
Washington, D. C. 2055
(202) 632-5965

NOTE: Sub-project is G-41-642

Assigned to: Applied Sciences

COPIES TO:

Project Director
Director, EES
Assistant Director
Division Chief
EES Accounting
Patent Coordinator

EES Supply Services
Security—Reports—Property Office
General Office Services
Library, Technical Reports Section
Office of Computing Services
Project File
Other Sue Corbin; Bonnee Wettlaufer

RA-3 (8-75)

SPONSORED PROJECT TERMINATION

Date: September 13, 1977

Project Title: Low Energy Experiment to Measure a Weak Coupling of the Neutrino Current

Project No: B-461

Project Director: T. P. Lang

Sponsor: National Science Foundation

Effective Termination Date: 6/30/77

Clearance of Accounting Charges: 6/30/77

Grant/Contract Closeout Actions Remaining:

- Final Invoice and Closing Documents
- x Final Fiscal Report (NSF Form 98)
- Final Report of Inventions
- Govt. Property Inventory & Related Certificate
- Classified Material Certificate
- Other _____

NOTE: Sub-project G-41-642/Ahrens/Physics had an effective termination date of 12/31/76. (Termination Sheet issued 3/30/77).

Assigned to: Applied Sciences Laboratory   (School/Laboratory)

COPIES TO:

Project Director
Division Chief (EES)
School/Laboratory Director
Dean/Director—EES
Accounting Office
Procurement Office
Security Coordinator (OCA) ✓
Reports Coordinator (OCA)

Library, Technical Reports Section
Office of Computing Services
Director, Physical Plant
EES Information Office
Project File (OCA)
Project Code (GTRI)
Other _____

CA—4 (3/76)

NATIONAL SCIENCE FOUNDATION Washington, D.C. 20550	SUMMARY OF COMPLETED PROJECT	Form Approved OMB No. 99R0013

Please read instructions on reverse carefully before completing this form.

1. INSTITUTION AND ADDRESS	2. NSF PROGRAM	3. GRANT PERIOD
Georgia Institute of Technology Atlanta, Georgia 31332	Nuclear Physics	1 Oct 75 – 30 Jun 77 *from* *to*

4. GRANT NUMBER PHY75-21295	5. BUDGET DUR. (MOS) 21	6. PRINCIPAL INVESTIGATOR(S) T. P. Lang & R. M. Ahrens	7. GRANTEE ACCOUNT NUMBER

8. SUMMARY (Attach list of publications to form)

The measurement of the cross section of the reaction $\bar{\nu}_e + d \to p + n + \bar{\nu}_e$, which proceeds only via the weak neutral current, has been experimentally determined to be feasible. The experiment requires several identical modules, each consisting of a central deuterated scintillator surrounded by a second lithium-6 loaded scintillator. All modules must be within a massive multilayered bulk shield which in turn is surrounded by an active scintillator anticoincidence cosmic ray shield.

First and second generation bulk and cosmic ray shields have been built and evaluated. A full size prototype deuterated scintillator module has been constructed and checked out, a reduced size lithium-6 loaded scintillator has been prepared and checked out and a full size dual concentric module has been constructed and evaluated. Experimentation has been concentrated upon the measurement of those factors affecting the counting time for the proposed experiment. Particular emphasis was directed at achieving an accurately calibrated low energy detection capability with absolute minimum background. The effects of cosmic rays, natural radioactivity and photomultiplier tube noise have been investigated extensively. The results are very encouraging and show that the counting time required for a measurement of the $\bar{\nu}(d,n+p)\bar{\nu}$ reaction cross section can be as short as 152 days.

Publications:
1. T. P. Lang, S. M. Blankenship, J. R. House, T. Ahrens, D. S. Harmer, M. H. Wood, and F. T. Avignone, III, "The Weak Neutral Current: A Low Energy Experiment," (Submitted for publication to SCIENCE.)
2. F. T. Avignone, III and Z. D. Greenwood, "The Weak Neutral Disintegration of the Deuteron by Reactor Antineutrinos," (Submitted to PHYSICAL REVIEW.)
3. F. T. Avignone, III and Z. D. Greenwood, "The Intepretation of $\bar{\nu}_e$-e$^-$ Scattering with Reactor Antineutrinos," Phys. Rev. (in press).

9. SIGNATURE OF PRINCIPAL INVESTIGATOR/ PROJECT DIRECTOR	TYPED OR PRINTED NAME T. P. Lang	DATE 8-18-77

NSF Form 98A (12-76) SUPERSEDES ALL PREVIOUS EDITIONS

Progress NR4—A

EES/GIT Project B—461

LOW ENERGY EXPERIMENT TO MEASURE A WEAK COUPLING OF THE NEUTRINO CURRENT

January 1977

1977

ENGINEERING EXPERIMENT STATION
Georgia Institute of Technology
Atlanta, Georgia 30332

Progress Report NR4-A
(EES/GIT Project B-461)

"LOW ENERGY EXPERIMENT TO MEASURE
A WEAK COUPLING OF THE NEUTRINO CURRENT"

Final Report, NSF Grant PHY75-21295

January 1977

Authors:

R. M. Ahrens
F. T. Avignone, III (Univ. S. Carolina)
S. M. Blankenship
D. S. Harmer
J. R. House
T. P. Lang
M. H. Wood

T. P. Lang
Project Director and
Principal Investigator
for Experimental Aspects

R. M. Ahrens
Principal Investigator
for Theoretical Aspects

GEORGIA INSTITUTE OF TECHNOLOGY

ATLANTA, GEORGIA

TABLE OF CONTENTS

LIST OF FIGURES

LIST OF TABLES

iv

ABSTRACT

The achievements of the Georgia Tech neutrino research group for the period October 1975 through December 1976 are described in this progress report. The goal of the present research activities is to perform an experiment in which features of the neutral weak current are investigated via the reaction of reactor antineutrinos with deuterons. The experiment requires several identical modules, each consisting of a central deuterated scintillator surrounded by a second lithium-6 loaded scintillator. All modules must be within a massive multilayered bulk shield which in turn is surrounded by an active scintillator anticoincidence cosmic ray shield.

First and second generation bulk and cosmic ray shields have been built and evaluated. A full size prototype deuterated scintillator module has been constructed and checked out, a reduced size lithium-6 loaded scintillator has been prepared and checked out and a full size dual concentric module has been constructed and is being evaluated. Experimentation has been concentrated upon the measurement of those factors affecting the counting time for the proposed experiment. Particular emphasis was directed at achieving an accurately calibrated low energy detection capability with absolute minimum background. The effects of cosmic rays, natural radioactivity and photomultiplier tube noise have been investigated extensively. The results are very encouraging and show that an upper limit for the counting time required for a measurement of the $\bar{\nu}(d,n+p)\bar{\nu}$ reaction cross section can be as short as 76 days.

Section A

INTRODUCTION

This report has been prepared for the National Science Foundation to document progress toward the goals of the neutrino research project at Georgia Tech. The ultimate goal of the present research program is to perform an experiment in which features of the neutral weak current are investigated via the reaction of reactor antineutrinos with deuterons.

This first year of our current effort has been devoted to establishing and examining the criteria bearing on the probable outcome or "feasibility" of the proposed experiment. Various prototype detectors were designed, constructed and evaluated. Particular emphasis was directed at achieving a low energy detection capability with absolute minimum background.

The project has moved along rapidly with gratifying progress. As originally proposed the experiment would be performed with six identical modules, each consisting of a central deuterated scintllator surrounded by a second lithium-6 loaded scintillator. All modules must be inside a massive multilayered bulk shield which in turn is surrounded by an active scintillator anticoincidence cosmic ray shield. First and second generation bulk and cosmic ray shields have been built and evaluated. A full size prototype deuterated scintillator module has been constructed and checked out, a reduced size lithium-6 loaded scintillator has been prepared and checked out and a full size dual concentric (but without lithium loading) module has been constructed and at this writing is being evaluated.

It had been our plan to build the first full size dual module complete with the capability of lithium loading. However, this would have entailed an extensive design, procurement and fabrication effort. Such an effort seemed inappropriate, since a possible significant improvement in the optimum size module became possible when it was discovered that 9" photomultiplier tubes are now available with adequate low noise and fast timing. This would allow the total number of modules for the experiment to be reduced from six to two! While a 9" diameter central module was being designed and fabricated it was decided to construct a full size dual module of plexiglass to evaluate the performance of the dual concentric configuration. Space limitations in the current shield dictated a design with a five inch diameter central detector and an overall diameter of nine inches. Besides, such a module, even without lithium loading,

will provide all of the data required to assess "feasibility" in terms of background effects.

Feasibility studies have been concentrated upon the measurement of those factors affecting the counting time for the proposed experiment. The effects of cosmic rays, natural radioactivity and electronic noise have been investigated by calculational techniques and experimentally with NaI detectors, neutron detectors and the prototype of the inner detector of the experimental module. The investigation of these effects with the prototype of a complete dual concentric detector module has begun.

A brief outline of the proposed experiment is presented in Section B along with a discussion of those factors bearing on the feasibility of the experiment. Sections C and D are devoted to the detailing of theoretical-analytical and experimental accomplishments.

A preliminary analysis of feasibility criteria established for the experiment is presented in Section E. These results are based on data collected with a full size dual concentric prototype module. This module was only recently completed and has been in operation less than a month; consequently the use of the word "preliminary". The results are very encouraging and show that an upper limit for the counting time required for a measurement of the $\bar{\nu}(d, n + p)\bar{\nu}$ reaction cross section can be as short as 76 days.

Section B

THE PROPOSED EXPERIMENT

Theoretical Background

While originally meant simply to establish the surmised (by the authors) existence of weakly interacting neutral currents, the experiment appears to be so well suited to measuring the pertinent axial vector coupling constant, that it continues to be of foremost interest even though neutral currents have been found at high energy.

Precisely what is to be measured is the axial vector coupling constant of the semileptonic weak interaction of neutral isovector currents. This is to neutral currents what the measurement of the (axial vector) coupling constant in, say, the beta decay of boron 12 is to charged currents. High energy neutrino experiments are clearly not as amenable to basic coupling constant determinations, since induced tensor interactions and momentum transfer dependent form factors get into the picture, in addition to both "basic interactions" (assuming that the basic neutral current interactions are of the vector and axial vector types).

As spelled out in the proposal, the deuteron disintegration at low energy involves only the isovector axial vector coupling constant, to an accuracy (of its square probably of better than 5 percent) that dispenses with the deuteron D-state admixture (the latter brings in the isoscalar axial vector coupling constant). Since the equilibrium reactor antineutrino spectrum is not quite that well known, this limitation is "academic". An overall accuracy of about 10 percent is the goal.

The originally theoretical idea of incorporating both deuterons and lithium-6 in a scintillator has been accomplished experimentally, although separately, and preferably so. This solution to the problem adds to the simplicity of the theoretical interpretation, since it should lead to practically complete recording of all nucleons from the deuteron disintegration.

Technical Approach

The technical approach, including the development and manufacture of special liquid scintillators, is the result of ten years of previous experimental investigations. As presently conceived, the experiment will consist of

six identical modules. Each module will contain two coaxial cylindrical scintil-
lation detectors, shown in schematic cross section in Figure 1.

This figure also illustrates the detection mechanism. The central scintil-
lator serves both as the target material and as the detector for the proton
resulting from the deuteron disintegration. The deuterons are substituted for
95 percent of the hydrogen normally present in the octane solvent. The reaction
product neutron migrates to the outer detector, which contains lithium-6. Upon
absorption of a neutron, the lighium-6 disintegrates into a triton and an alpha
particle, with a minimum total kinetic energy of 4.8 MeV. The temporal and
spatial distribution functions displayed in Figure 2 illustrate the timing
requirements for the event signature and the dimensional requirements for de-
tector size. These distributions were obtained by multi-region Monte Carlo
neutron transport calculations. The chemical compositions of the two special
liquid scintillators developed for this experiment are given in Tables I and II.

TABLE I.   COMPOSITION OF DEUTERATED SCINTILLATOR

Chemical Name	Formula	Molecular Weight	% By Weight
deuterated n-octane	$CD_3(CD_2)_6CD_3$	132	93.2
deuterated naphthalene	$C_{10}D_8$	136	2.4
bis-MSB	$C_{24}H_{22}$	310	0.01
PPO	$C_{15}H_{11}NO$	221	0.4
n-octane	$CH_3(CH_2)_6CH_3$	114	3.9
naphthalene	$C_{10}H_8$	128	0.1

ATOMIC COMPOSITION

H	32.1	$\times 10^{20}$	ATOMS/cm^3
D	646.	"	"
C	308.	"	"
N	0.091	"	"
0	0.091	"	"

Density = 0.833 g/cm^3

DETECTION SCHEME

LOW ENERGY EXPERIMENT TO MEASURE A
WEAK COUPLING OF THE NEUTRINO CURRENT

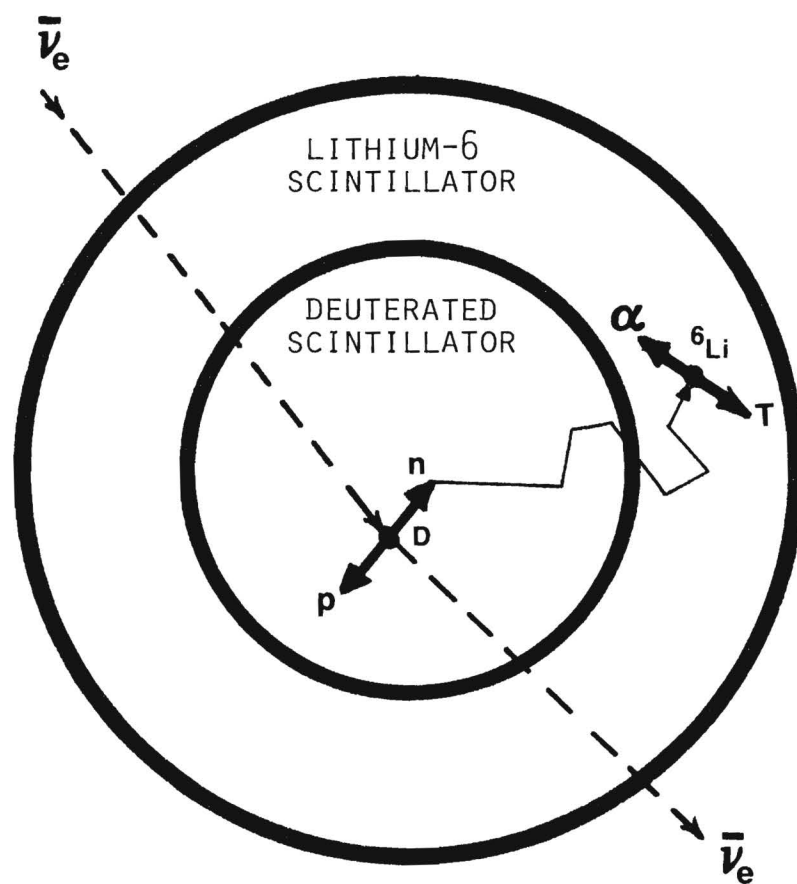$$\bar{\nu}_e + D \longrightarrow P + N + \bar{\nu}_e$$
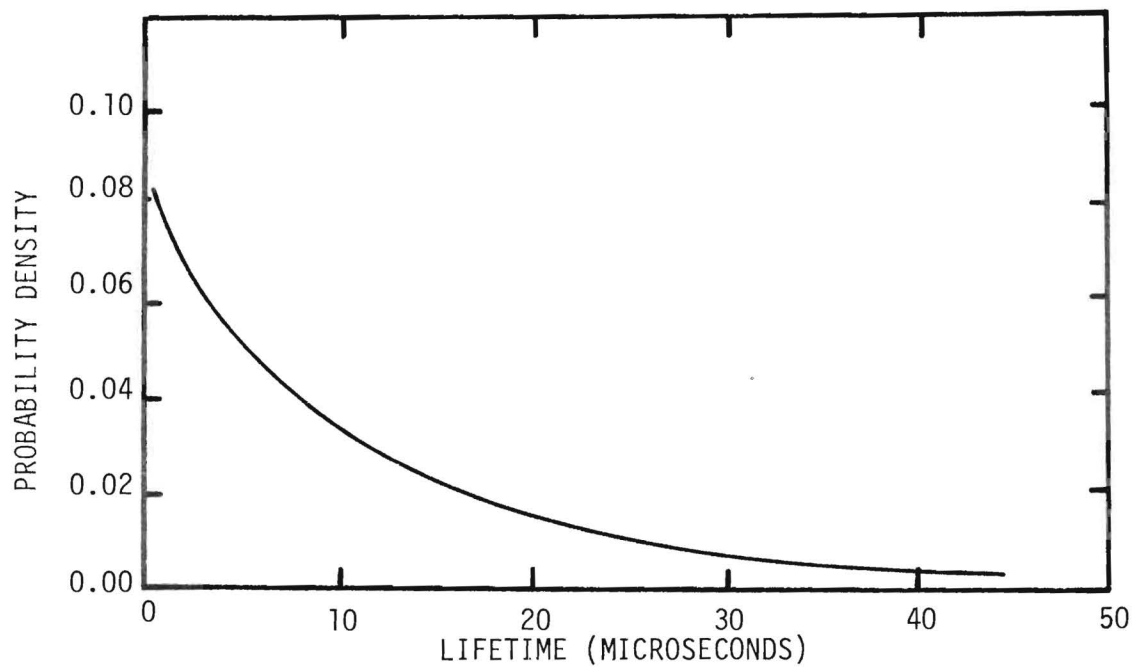

FIGURE 1. DETECTION SCHEME

FIGURE 2a.   TEMPORAL PROBABILITY DENSITY FUNCTION FOR NEUTRON CAPTURE
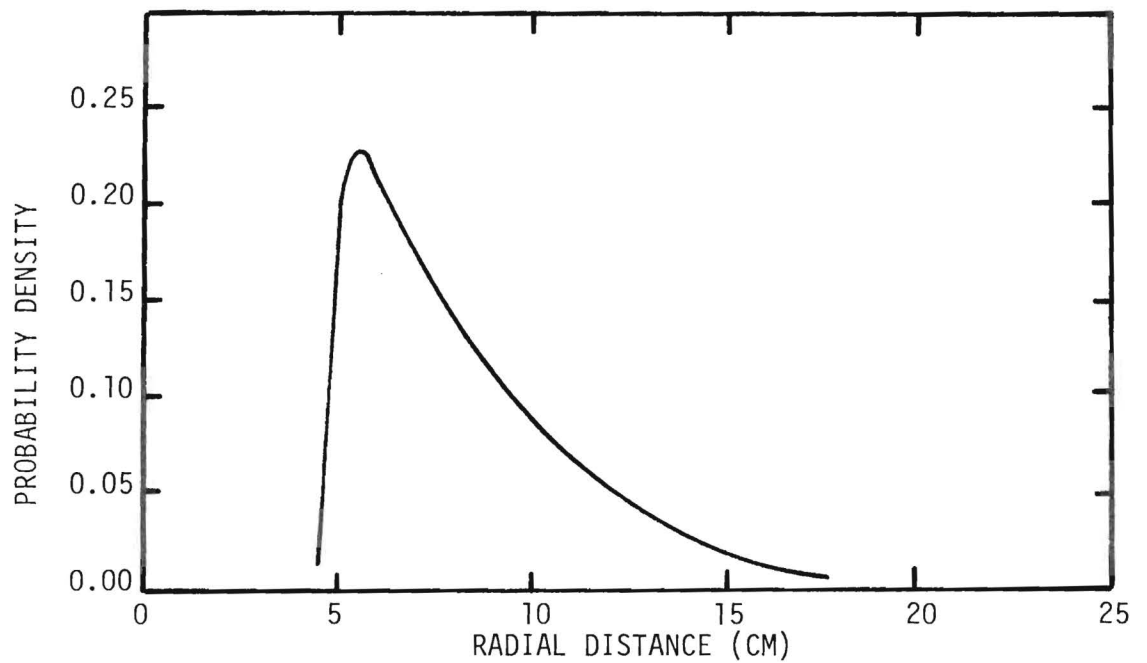

FIGURE 2b.   SPATIAL PROBABILITY FUNCTION FOR NEUTRON CAPTURE

6

TABLE II. COMPOSITION OF LITHIUM-6 LOADED SCINTILLATOR

Chemical Name	Formula	Molecular Weight	% By Weight
phenylcyclohexane	$C_6H_5C_6H_{11}$	160	89.1
PPO	$C_{15}H_{11}NO$	221	0.4
bis-MSB	$C_{24}H_{22}$	310	0.01
naphthalene	$C_{10}H_8$	128	2.5
^{6}Li-butoxide	$^6LiOC_4H_9$	79	7.5
^{7}Li-butoxide	$^7LiOC_4H_9$	80	0.5

ATOMIC COMPOSITION

H	637.6	$\times 10^{20}$	ATOMS/cm^3
^{6}Li	6.0	"	"
^{7}Li	0.4	"	"
C	466.	"	"
N	0.12	"	"
O	6.5	"	"

Density = 1.059 g/cm^3

The antineutrinos will be provided by the fission product decays at a large nuclear reactor. To achieve maximum antineutrino fluxes, the experiment must be as close as possible to the core of such a reactor. Given a knowledge of the antineutrino spectral flux from fission product decays at the experimental site and the variation of the deuteron disintegration cross section with energy, the kinetic energy distributions for breakup nucleons are calculable. These energies allow a restriction of the energy range of interest in the proton detector. They also allow a calculation of the time spent by the neutron between creation and absorption by lithium-6, about 90 percent being captured within 33 microseconds. The lithium-6 disintegration occurs with a relatively delimited energy.

The signature for the observation of an antineutrino disintegration event is a pulse in the proton detector corresponding to an energy that the proton is likely to possess, followed within 33 microseconds by a lithium-6 breakup in the outer detector. Massive shielding and other techniques are utilized to reduce the rate of background processes which can mimic this signature.

The expected event rate can be calculated from the product of the antineutrino flux (3.0×10^{13} antineutrinos per square centimeter per second), the cross section (predicted to be 0.65×10^{-44} square centimeters), and the number of target deuterons in forty liters of deuterated scintillator (2.56×10^{27} nuclei). This product is 1.8 events per hour. The observed rate is expected to be the product of this and the efficiency for observing the event signature, 0.5. The expected observed signature event rate is 0.9 counts per hour.

Feasibility Criteria

There are several sources of background events which can contribute to the observed signature event rate. These are:

1. the reactor, which produces neutrons and gamma rays as well as antineutrinos at the experimental site,

2. natural radioactive contamination,

3. cosmic rays, which have a soft and hard component, and

4. electronic noise, particularly that originating in the photomultiplier tubes.

The particles produced by these sources and the spurious pulses of electronic noise can produce signatures which are indistinguishable from the antineutrino induced disintegration of the deuteron. Some of these are the result of correlated events in the detectors, and some are the chance synthesis of the event signature. The chance synthesis will be seen to be the most significant source of interferring background.

The correlated events consist of the following:

$$^{2}\mathrm{H}\ (n,n)\ ^{2}\mathrm{H} \tag{1a}$$

$$^{2}\mathrm{H}\ (n,2n)\ ^{1}\mathrm{H} \tag{1b}$$

$$^{1}\mathrm{H}\ (n,n)\ ^{1}\mathrm{H} \tag{1c}$$

$$^{2}\mathrm{H}\ (\gamma,n)\ ^{1}\mathrm{H} \tag{1d}$$

$$\star \quad ^{2}\mathrm{H}\ (\bar{\nu},\bar{\nu}n)\ ^{1}\mathrm{H} \tag{1e}$$

8

$$^2H \ (\bar{\nu}, e^+) 2n \qquad\qquad\qquad\qquad (1f)$$

$$^1H \ (\bar{\nu}, e^+) \ n \qquad\qquad\qquad\qquad (1g)$$
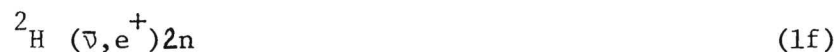
Each of these reactions, if it occurs within the inner detector, produces a charged particle in the inner detector and at least one neutron. Only reaction (1e) is the desired event. The others are capable of mimicing the same signature. Background signature events may also be synthesized by such processes as the multiple scattering of gamma rays between detectors. Such events may be distinguished from genuine signature events by the short times between the two scatterings. The discrimination against all these sources of correlated background signatures will be accomplished as indicated below.

Synthesis of the signature can occur by the uncorrelated chance ocurrence of delayed coincident events in both detectors. The rate of chance signature synthesis is reduced by reductions in the single event rate in each detector.

The reactor associated signature event rate S is given by

$$S = R_u - R_d \qquad\qquad\qquad\qquad (2)$$

where R_u and R_d are the observed signature event rates with the reactor "up" and "down", respectively. The passive shield for the proposed experiment has been designed to limit the reactor associated correlated synthetic event rate from reactions (1a), (1b), (1c) and (1d) to less than ten percent of the expected genuine event rate. (T. P. Lang and R. M. Ahrens, Advanced Research Corporation Technical Reports NR1-H, "Detector Shielding," and NR2-C, "Experiment Shielding".) Other investigators have achieved similar results with passive shields. (Cf F. T. Avignone, III and C. W. Darden, NUCLEAR INSTRUMENTS AND METHODS 96 (1971), p. 343.) The reactor associated antineutrino induced background events, (1f) and (1g), may be discriminated against by their unique features. The cross section of reaction (1f) will cause a reduced event rate compared to reaction (1e). The positron energy will distinguish it from most of the protons of reaction (1e). The capture of both neutrons of reaction (1f) will further distinguish it from (1e). The almost complete deuteration of the target scintillator will strongly inhibit reaction (1g) (as well as reaction (1c)). The rate S will then represent essentially the interaction of interest, (1e).

Given unlimited time, the passive shield would allow the measurement of S to any required precision. The resources of the experimenter and the stability of the instrumentation over long periods place practical upper limits upon the counting time. An expression is derivable from equation (2) which will allow an estimate of the counting time and illustrate the methods suited to its reduction.

Let the criterion for a statistically significant signal be

$$S = k \, \sigma, \tag{3}$$

where σ is the uncertainty in S, and k is a number which determines the desired precision. If we assume that counting uncertainties are the major contributors to σ, then we can calculate the time required to perform the experiment. If C is the number of signature events observed with the reactor not operating during a time T, then

$$R_d = C \, / \, T, \text{ and } \sigma_d = C^{\frac{1}{2}}/T, \tag{4}$$

where σ_d is the uncertainty in R_d. Equal statistical uncertainties in R_d and R_u require the same counting times for each, because typical conditions for this type of neutrino experiment imply near equality of R_d and R_u. Thus,

$$R_u = C \, / \, T, \text{ and } \sigma_u = C^{\frac{1}{2}}/T, \tag{5}$$

where σ_u is the uncertainty in R_u.

The uncertainty in S, the square root of the sum of the squares of σ_d and σ_u, is then given by

$$\sigma = (2 \, R_d \, / \, T)^{\frac{1}{2}}. \tag{6}$$

Combining equations (3) and (6) and solving for T yields

$$T = 2 \, R_d \, (k/S)^2. \tag{7}$$

It is apparent from equation (7) that an efficient method of decreasing T is to increase S. The amount of target material available is limited to 40

liters, and the antineutrino flux is determined by the selection of the experimental site. Increasing the efficiency of detection of the reaction products would also increase S, but the present total efficiency (about 0.5) is already quite good and an improvement cannot provide orders of magnitude reduction in T. The reduction of R_d is the other alternative. The sources of pulses contributing to R_d are natural radioactive contamination, cosmic rays and electronic noise.

One of the major limiting factors in any low level counting experiment is the radioactive contamination and/or internal radionuclide content of the detector components and shielding. Among the most often troublesome radionuclides are potassium-40, the uranium and thorium decay chain products, and fallout. By virtue of their raw materials and methods of manufacture, the scintillation liquids and the plexiglass containment vessels are relatively uncontaminated. All materials inside the passive shield are carefully selected for low contamination.

The cosmic ray flux consists of a soft component and a penetrating component. The soft component, consisting of electrons, photons and slow muons, is eliminated by the passive shield. The penetrating component striking the detector will in general deposit a large amount of energy in the detector and can be effectively discriminated against on the basis of pulse amplitude. An anticoincidence umbrella detector system reduces the effects of secondary particles created by the cosmic rays within the shield.

Interferring electronic noise pulses are limited to those which originate in the photomultiplier. This effect is controlled by the use of low noise photomultiplier tubes, and by the use of two photomultiplier tubes viewing each detector in coincidence. The noise pulses are random, and the coincidence requirement strongly favors pulses originating in scintillation events in the detector.

The effect upon the counting time T of gamma rays from natural radioactivity and other sources within the shield due to reaction (1d) can be estimated. This effect is treated in Section C and shown not to limit feasibility. The only source of non-reactor associated neutrons is cosmic ray secondaries. The flux of the hard component of the cosmic rays is about one per minute per square centimeter. The flux of gamma rays at all energies can exceed one per second per square centimeter in an unprotected detector. Given these fluxes one

11

expects the effects of reactions (1a), (1b) and (1c) to be even less significant. The synthetic events involving the prompt scattering of particles such as gamma rays from one detector to the other so as to produce the event signature can be rejected by their prompt time relationship.

The magnitude of the particle fluxes and the magnitude of typical photo-multiplier tube noise pulse rates suggests the possibility that they are capable of producing significant signature rates by pure chance. The effects upon T of this chance signature event rate must be quantified. Only a measuremant of these chance rates can quantify their effect upon R_d and T. For this reason, the study of the sources of these events and their reduction is the main goal of the present feasibility study. The nature and effect of cosmic ray produced correlated events is an important secondary goal of the study.

Section C

THEORETICAL/ANALYTICAL PROGRESS

Theoretical Studies

Attempts are under way at deriving tractable expressions for the actual (as distinguished from "reduced") nucleon spectra resulting from the deuteron disintegration by equilibrium reactor antineutrinos. Knowledge of this spectrum could be beneficial to the interpretation of delayed coincidence measurements of proton and neutron capture pulses.

Some basic studies are under way concerning massless particles and their differences from massive particles, particularly from the standpoint of group and gauge theory. Such views become particularly pertinent when deviations of the neutrino mass from zero are considered.

Possibilities for further low energy neutrino experiments, e.g. as involving other coupling constants, are being examined.

Reactor Antineutrino Spectra

The spectrum of antineutrinos from a fission reactor commonly used was calculated in 1970 (F. T. Avignone, III, PHYS. REV. D2, 2609, 1970). The calculation was made from experimental determinations of fission mass yields, charge distributions and information regarding the beta decay of the fission products. The 1970 spectrum was based on spectroscopy data available through 1969 and involved a total of 548 beta decay branches. Only 260 of these were found in known decay schemes. The pertinent information regarding the unknown decay schemes was calculated from empirical mass formulas and by extrapolation of general features of known decay schemes.

A recalculation of the spectrum appears justified by the significant number of new decay schemes as well as developments in mass formulas since 1970. Our knowledge of the charge distributions has not changed significantly during the past six years.

Photodisintegration of the Deuteron

One source of background which will be indistinguishable from the antineutrino disintegration of the deuteron is the photodisintegration of the deuteron by the ambient gamma ray background. The well known analytical expressions for the photodisintegration cross sections associated with the electric

13

and magnetic dipole absorption modes may be combined to allow a calculation of the total event rate given the gamma ray spectral flux. A careful evaluation of the interference from this source of events is necessary to insure that an accurate cross section measurement for the antineutrino deuteron disintegration process is feasible.

The present evaluation is based on the gamma ray flux measured inside Shield II. The measurements were made with a 3" x 3", NaI detector. Hence the question of detector response and its distortion of the gamma ray spectrum is a very important one.

The final photodisintegration rate observed in the inner portion of the dual-region detector is given by

$$R(events/day) = <\sigma> \ (events/sec \cdot deut) \ x \ (8.64 \ x \ 10^{4} \ sec/day)$$

$$x(6.5 \ x \ 10^{25} \ deut/liter) \ x \ (40 \ liters). \tag{8}$$

The quantity $<\sigma>$ is the effective cross section given by

$$<\sigma> \ = \ \int \Phi(E_\gamma) \ \sigma(E_\gamma) \ dE_\gamma \ , \tag{9}$$

where $\Phi(E_\gamma)$ is the measured gamma ray flux and $\sigma(E_\gamma)$ is the theoretical total cross section for photodisintegration of the deuteron.

The total theoretical cross section $\sigma(E_\gamma)$ is made up of two contributions, namely the electric dipole and the magnetic dipole absorption of the photon. The well known electric dipole contribution is given by Evans (R. D. Evans THE ATOMIC NUCLEUS, McGraw-Hill Book Company, Inc., New York, 1955). in the following form:

$$\sigma(E1) \ = \ \frac{8\pi \ \rho^{2}}{3(137)} \left[\frac{\sqrt{B(h\nu-B)}}{h\nu} \right]^{3} \{1 - {^3}r_{o}/\rho\}^{-1} \ , \tag{10}$$

where ${^3}r_{o}/\rho = 0.394$, $\rho = \hbar / \sqrt{2mB} = 4.31 \ x \ 10^{-13} cm$, and $B = 2.225$ MeV, the binding energy of the deuteron bound state. In addition Elton (L. R. B. Elton, NUCLEAR THEORY, W. B. Saunders, Company, Philadelphia, 1965) gives the following expression for the ratio $\sigma(E1)/\sigma(M1)$:

14

$$\sigma(E1)/\sigma(M1) \quad = \quad 70 \times E(E + |B_s|)/(E + B)^2, \tag{11}$$

where B_s is the binding energy of the unbound singlet state of the deuteron (+0.070 MeV) and E is the energy of the final state of the nuclear system (hν-B). If we evaluate the constants and combine equations (10) and (11), we arrive at the following expression for the total photodisintegration cross section:

$$\sigma(E_\gamma) \quad = \quad (1.874 \times 10^{-26} \text{cm}^2) \left[\frac{\sqrt{B(E_\gamma - B)}}{E_\gamma} \right]^3 \left[1 + \frac{E_\gamma}{70(E_\gamma - B)(E_\gamma - B + |B_2|)} \right]. \tag{12}$$

A plot of this cross section is given in Figure 3. Also one can compare Figure 3 with Figure 4.1 of Evans in which $\sigma(E_\gamma)$ is also compared with the experimental cross sections.

The photon flux $\Phi(E_\gamma)$ is not nearly so easy to obtain as the cross section $\sigma(E_\gamma)$, since the response of the 3" x 3" NaI detector is extremely complex. A complete theoretical analysis of this response for a 3" x 3" NaI detector which is based on a complex Monte Carlo calculation has been initiated; however, strong evidence exists that a reasonably accurate evaluation of equation (9) can be accomplished, for the present, with far less effort. The fact that this is true at the energies of interest above 2 MeV, while it is well known not to be true below 1 MeV, can be seen by considering the spectrum shown in Figure 31 of Shaforth (S. M. Shaforth, SCINTILLATION SPECTROSCOPY OF GAMMA RADIATION, Gordon and Breach Science Publishers, New York, 1967). At these higher energies the full energy peak is dominated by pair creation and seriously broadened by the single and double annihilation radiation escape peaks. The scattering distribution throughout most of the energy range of interest is a small, almost flat distribution running down to zero energy. The ratio R of the scattering cross section and the total absorption is plotted in Figure 4. One can see immediately that the ratio σ_s/σ_{ab} above 2.225 MeV, the photo-disintegration threshold, is vastly smaller than it is in the vicinity of 1 MeV. We have estimated the distortion effect of the scattering continuum on the gamma ray spectrum by approximating the detector response above threshold with a 1 MeV wide, flat, full-energy distribution followed by a flat tail which has an integral chosen so that its ratio with the integral under the full energy distribution is given by σ_s/σ_{ab}. (See Figure 5.) The observed spectrum was
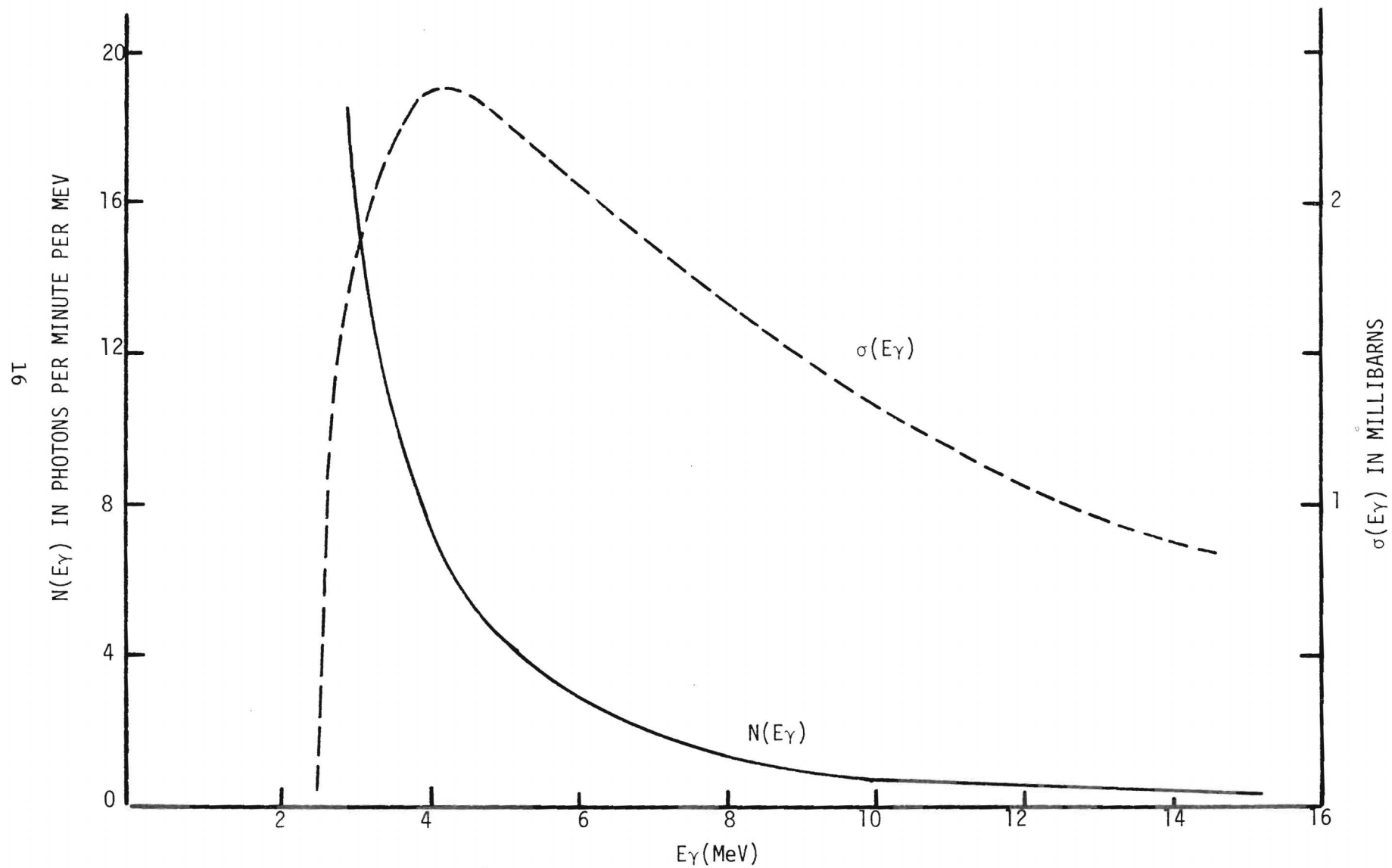
15

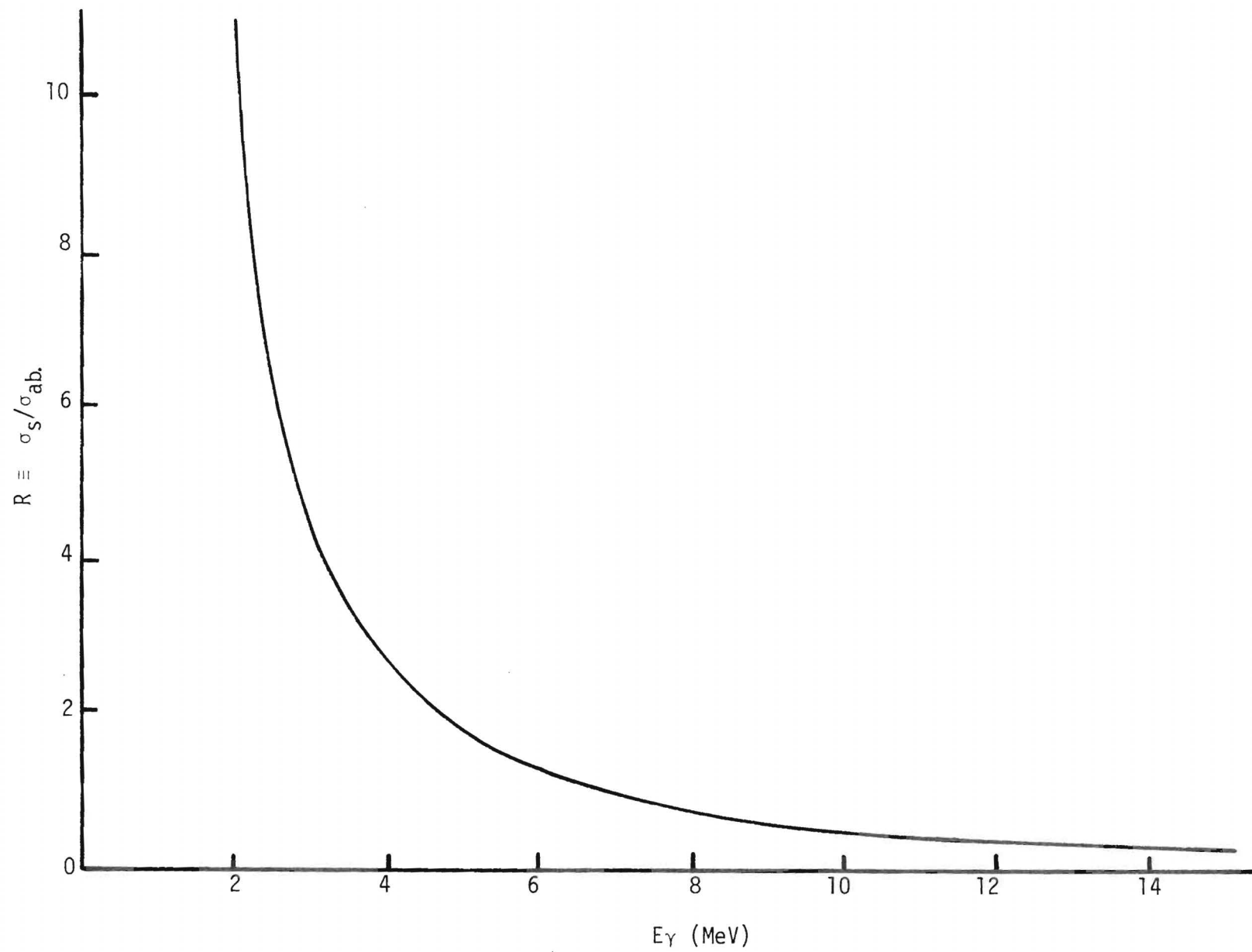FIGURE 3. BACKGROUND GAMMA RAY SPECTRUM AND PHOTODISINTEGRATION CROSS SECTION

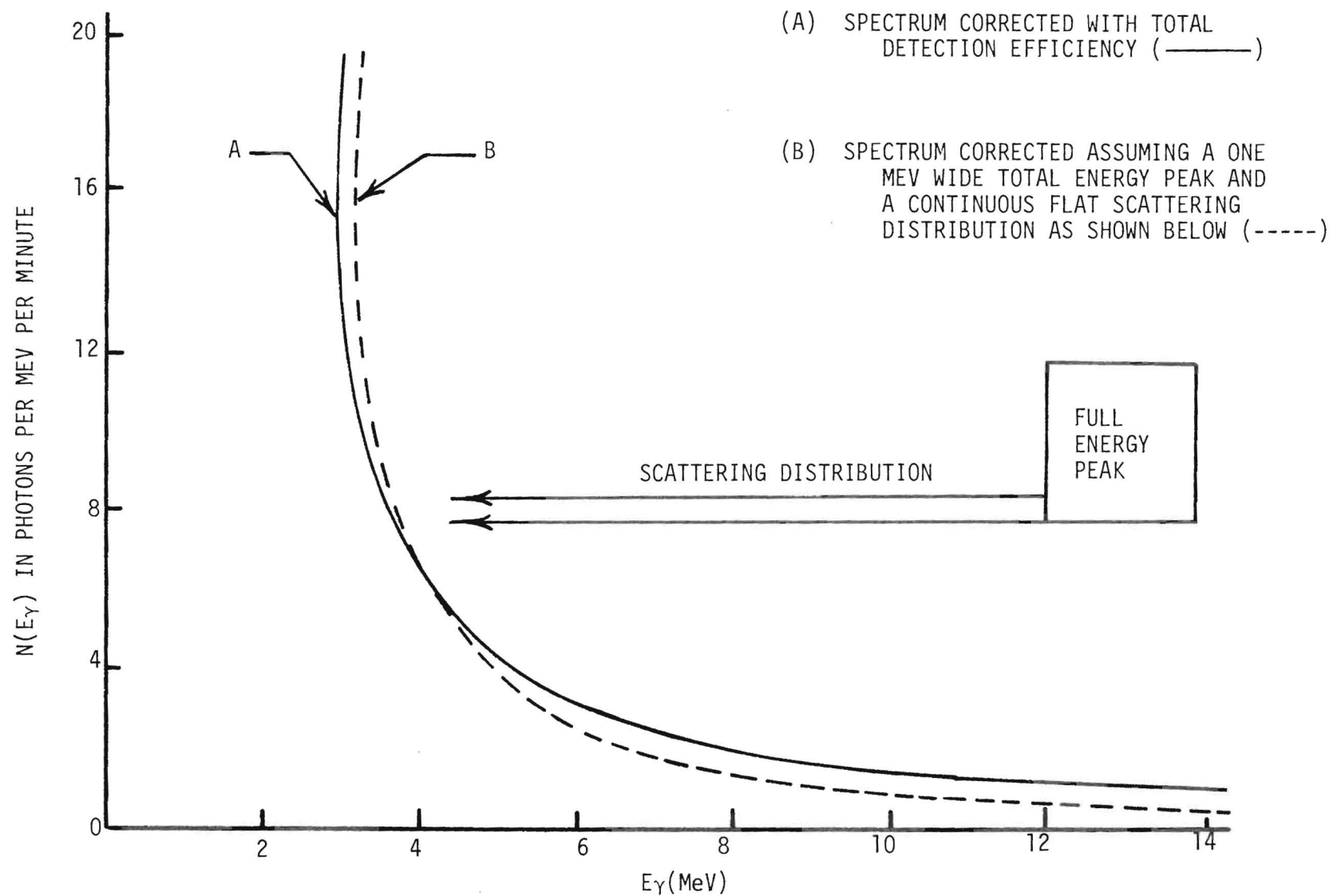FIGURE 4.   NaI GAMMA RAY CROSS SECTION RATIO

FIGURE 5. GAMMA RAY SPECTRA

then corrected by calculating the tail of the highest energy region, subtracting it from all of the lower intervals and adding it to the highest one. The next lowest interval then presumably contains no scattering contribution and its scattering distribution was calculated with σ_s/σ_{ab} at that energy and from this ratio, the flat scattering continuum was calculated and subtracted from all lower intervals. This procedure was repeated until the lowest energy interval was corrected. The cross sections and absorption coefficients used throughout this analysis were taken from the work of Hubbell (J. H. Hubbell, National Stand. of Ref. Data Ser. 29, 1-80, 1969). The result of this crude calculation is shown in Figure 5. As can be seen, in the first approximation the spectral distortion at energies between 2.25 and 15 MeV are far less important than they are at low energies.

A more complete analysis of the distortion characteristics of a 3" x 3" NaI detector is very complex and is presently underway. While most of the required computer subroutines have been written, a great deal of development time will have to be invested. The crucial test of such a Monte Carlo code will be its ability to reproduce the observed spectrum of a known gamma ray spectrum. While response matrices of such detectors have been obtained quasi-experimentally, a search of the literature indicates that no such response matrices exist for the energy range of interest and for the case in which gamma rays enter the detector from completely random directions incident at points which are chosen completely randomly.

The spectrum (A) in Figure 5 is considered to be the zero order approximation to the actual spectrum and was obtained by simply correcting each point in the observed spectrum by dividing through by the total detection efficiency. This efficiency was calculated using a Monte Carlo code which chooses random entry and exit points on the sphere circumscribing the cylindrical detector and connects these points with a straight line. The trajectory distance d through the crystal is calculated and the quantity $(1-e^{-\mu d})$ is computed which is the probability of interaction since μ is taken to be the total absorption coefficient in cm^{-1}. A random number is then selected on the interval (0,1) and compared to $(1-e^{-\mu d})$. If the random number is the lesser, the event is registered as an interaction. The fraction of trajectories through the sphere which also penetrate the cylindrical detector is also computed for use in the calculation of the gamma ray flux. The basic area used in the flux calculation is then the projected area of the sphere. The fraction of random, straight

line trajectories which pierce both the 3" x 3" diameter cylinder and the circumscribing sphere is found by the Monte Carlo method to be 0.785. The table of total efficiencies is given below in Table III. The flux as a function of energy is then given in the present approximation by,

$$\Phi(E_\gamma) = N(E_\gamma) \left[(\pi R_s^2) \; P(E_\gamma)(0.785) \right]^{-1} \tag{13}$$

where R_s is the radius of the sphere which circumscribes the cylindrical 3" x 3" NaI detector. This flux was then multiplied by $\sigma(E_\gamma)$ and integrated over all energies from threshold up. The result of equation (13) was thus found to be 659 deuteron photodisintegrations per day in the 40 liter inner region of the coaxial detector. While this may seem to be a very large number, a statistical analysis presented later in this report shows that this source of background adds 21 counting days to the proposed measurements. We consider this value to be ± 20% of what a far more sophisticated analysis of the gamma ray spectrum would yield or that which the planned direct measurement will yield. In addition, it is shown below that while this background rate is significant, it does not represent a crippling obstacle to the planned cross section measurements.

TABLE III.
PROBABILITY OF DETECTING RANDOMLY ORIENTED GAMMA RAYS BY 3" x 3" NAI CRYSTAL

E_γ (MV)	$P(E_\gamma)$	E_γ (MeV)	$P(E_\gamma)$
1	.0730	5	.4750
2	.5700	6	.4890
3	.5400	8	.5000
4	.4850	10	.5280
		15	.5500

Section D.

EXPERIMENTAL PROGRESS

Apparatus And Calibration

Data Collection

The more important data presented in this report are scintillation pulse height spectra. The detectors consisted of NaI and LiI inorganic scintillators, and various organic liquid scintillators. Typical electronics are shown schematically in Figure 6 which illustrates the electronics necessary to provide an analog sum signal in fast coincidence between two photomultiplier tubes observing the same liquid scintillator. The solid scintillators were observed with only one photomultiplier tube, so that only one half of the signal processing electronics was required. The use of the gating signal, in either coincidence or anticoincidence, was switch selectable for all detectors.

Energy calibration of the inorganic scintillators was accomplished by observation of the photopeaks from decay gamma rays. Energy calibration of the octane based and lithium-6 loaded liquid scintillators was obtained from measurements of Compton edges of decay gamma rays. Intermediate energies were interpolated by straight line methods. Electronic linearity was determined by substituting a calibrated pulser for the photomultiplier tubes. The pulse height corresponding to zero energy deposition was determined by extrapolation of the pulser linearity calibration to zero. The cosmic ray umbrella detectors were calibrated to assure that the discriminator settings were well below the cosmic ray "through peak".

For those scintillators which were observed by more than one photomultiplier tube, the tubes were balanced, that is, adjusted to produce equal pulse heights for the same deposited energy. Equal energy deposition was obtained from a gamma ray source irradiating the center of the detector or from the cosmic ray through peak. Gains of the individual tubes were adjusted to give equivalent outputs. The times of arrival of the analog pulses from the photomultiplier tubes were adjusted so that appropriate sums were obtained.
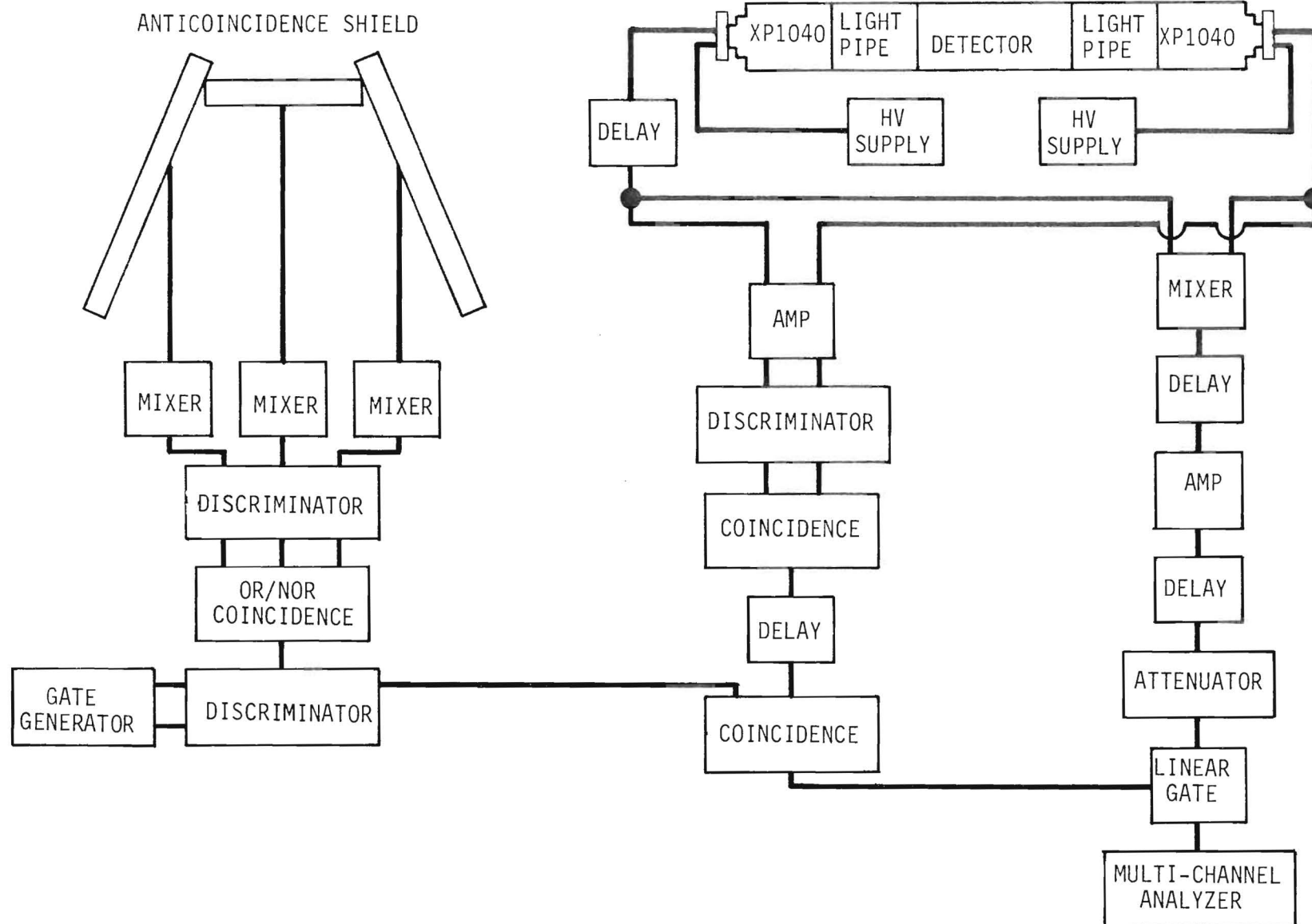
FIGURE 6. SCHEMATIC TYPICAL OF EXPERIMENTAL ELECTRONICS

22

All coincidence or anticoincidence requirements necessitated precise timing of the gating signals. The timing of signals from photomultiplier tubes observing the same scintillator was accomplished by irradiating the scintillator with gamma rays. This insured that all the signals began within the spread of the light collection times, typically a few nanoseconds. The timing of cosmic ray umbrella pulses with respect to associated pulses from a detector inside the shield was accomplished from the through peak in both detectors, which added the slight additional spread and delay associated with the flight times of cosmic rays through the shield. The determination of proper timing was made by one of three methods. One displayed the time relationship of various signals on a fast oscilloscope. Another was to count coincidence rates as various delays were introduced into the system, with the delays associated with maximum rate representing appropriate timing. The last method employed a time to amplitude converter.

The widths of timing and logic pulses were also investigated. Most such widths were adjusted to be long enough to allow true signals to pass and short enough to discriminate against the inclusion of noise pulses in the analog signal. Typically, these widths were a few tens of nanoseconds. The width of the umbrella gating pulse was the subject of a separate determination. It was in general longer, typically of the order of a few microseconds.

From the pulse height spectra collected with the multichannel analyzer, such data as rates and energies were obtained. Counts within peaks were obtained by subtracting background over the peak width. The background was usually assumed to be linear. When it was obviously steeply rising at low energies, an exponential background was assumed.

Rates within energy windows were obtained from the sums of included counts without background subtraction. The proton energy window was 0.1 to 1.0 Mev, or 0.013 to 0.130 Mev electron equivalent energy. The neutron window was established directly from the calibration of the neutron detector with the neutron source, and included 0.3 to 0.75 MeV electron equivalent energy. (See below for a disucssion of electron equivalent energies.)

Monte Carlo Calculation of Scintillator Response

To aid in the correlation of the shape of the observed liquid scintillator spectra with gamma ray energy, particularly at low energy, and to aid in determining system resolution, a computer program using Monte Carlo

techniques was written. It permits calculation of the energy deposited in a cylindrical, octane based liquid scintillator by a monoenergetic gamma ray source. The source may be located at an arbitrary point on the surface of the cylinder, and its energy between 0.01 and 1.0 MeV. Given the relative magnitudes of the cross sections for carbon and hydrogen, and the relative densities of octane and solutes, carbon is the only appreciable contributor to the gamma ray-scintillator interaction.

The program allows calculation of the spectrum of energy deposited in the scintillator to within desired statistical uncertainties. The program will be expanded to allow a wider range of experimental conditions, such as the location of the source at an arbitrary point in space and the inclusion of the outer detector of the two detector module. The introduction of resolution functions will allow a comparison of the calculated energy depsoition spectra to the experimentally observed pulse height.

Scintillator Chemicals and Response

The energy of the proton and neutron are important parameters of the signal signature. Consequently, the response of scintillators as a function of energy for these particles must be examined. It was possible to develop scintillators with a large light output for a given deposited energy. This results in improved resolution and aids the discrimination between scintillator output and electronic noise.

The response of scintillators to particles other than electrons is usually defined by comparison to the electron response. Over the ranges of energy involved in this experiment, the response of the liquid scintillators to electrons is linear, with a slight deviation from linearity at the lowest energies. The introduction of monoenergetic electrons directly into the scintillator would provide a useful benchmark, but several practical considerations preclude the use of this technique. Dissolving a source of monoenergetic internal conversion electrons is difficult to repeat frequently and would ultimately degrade the performance of the scintillator. The introduction of a beam of low energy electrons from outside the cell is unsuitable, because there are effects caused by the cell walls.

The standard method of calibrating scintillators by photo peaks is not applicable to inorganic liquid scintillators, for photo peaks are unobservable.

24

Irradiation of the scintillator with gamma rays will produce Compton recoil electrons. This avoids edge effects, but the energy distribution of such electrons is not simple. In large liquid scintillators, the probability of multiple scattering without total absorption further confuses the interpretation of the response. These difficulties may be surmounted. The energy distribution of Compton electrons as a function of gamma ray energy is well known. The effects of scintillator resolution and size can be calculated. The use of gamma ray sources to calibrate liquid scintillators and to monitor their performance is simple to perform, usually safe for both the experimenter and the scintillator, and, for these reasons, traditional.

To determine the scintillator composition which yields the optimum response, comparisons were made among samples with differing compositions. Pulse height spectra were collected with the scintillator samples in a standard 10 ml. test cell, irradiated by a cesium-137 gamma ray source. The pulse height spectra from the scintillator samples were compared with that of NE213, a standard commercial liquid scintillator. From these results and the previous studies with larger volumes, the optimum concentrations of 0.4% PPO, 0.01% Bis-MSB, and 2.5% naphthalene in an n-octane solvent were determined. This mixture gives an output which is 81% that of NE213. By comparison, the mineral oil based scintillator used in the cosmic ray umbrellas has a response which is 64% that of NE213.

A six liter cylinder, viewed through light pipes by two photomultiplier tubes, was filled with this scintillator. Figures 7 and 8 show the pulse height spectra obtained when this cell was exposed to the decay gamma rays of manganese-54 (0.84 MeV) and cesium-137 (0.66 MeV). The Compton "edges" are present, although smeared by the effects of multiple scatterings and the system resolution. They provide markers by which electrical responses from the detector are associated with electron energy.

The response of the sintillator to very low energy gamma rays was investigated by the use of the 29 keV x-ray in the decay of cadmium-109. The response of the scintillator is complicated by the presence of many multiple scatterings at such low energies. From the observed rate, electron energies at least as low as 18 keV have been identified. The completion of the Monte Carlo computer calculation of the response of the scintillator to gamma rays will aid a more precise interpretation of the low energy calibration results. The identification
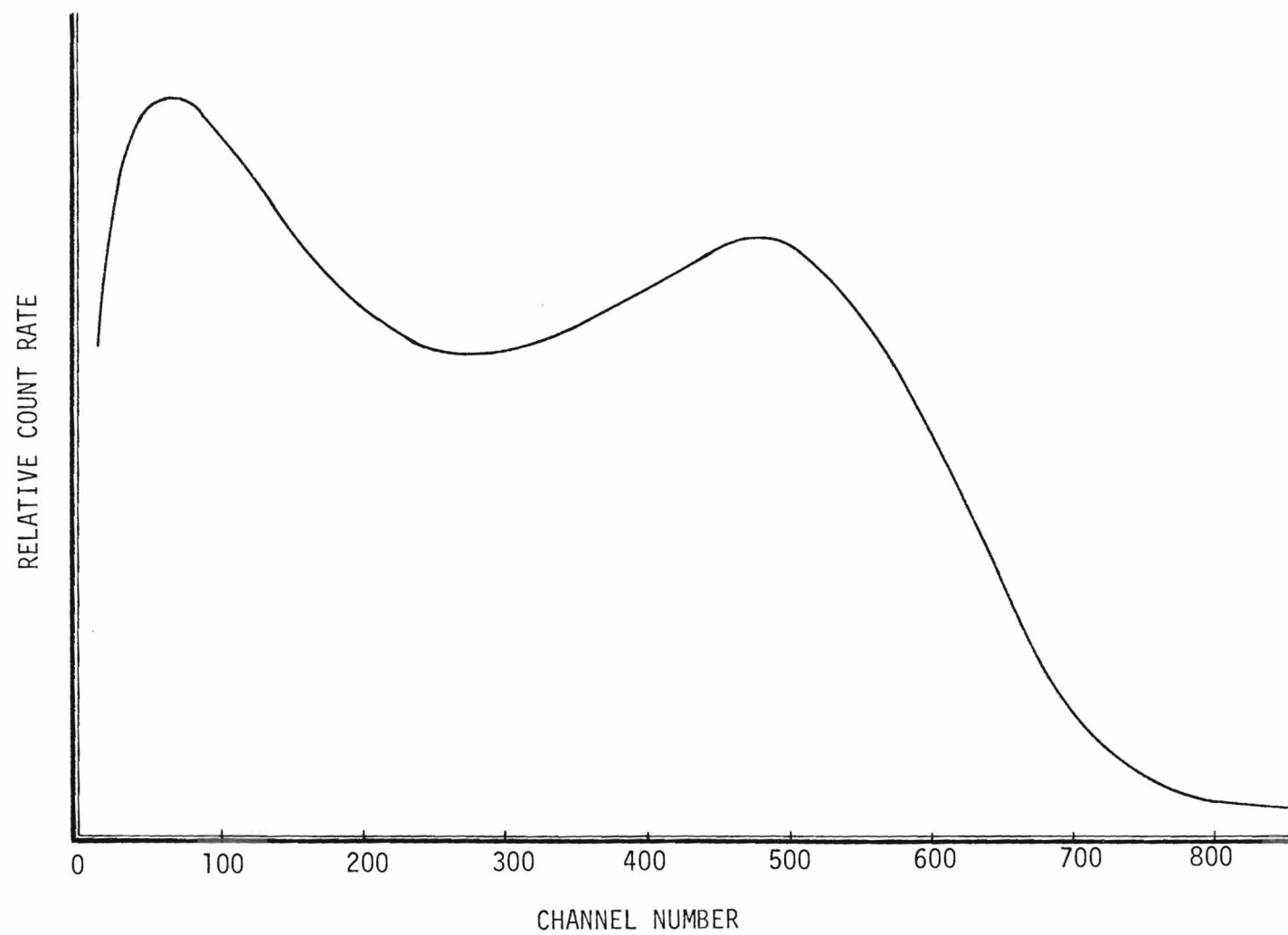
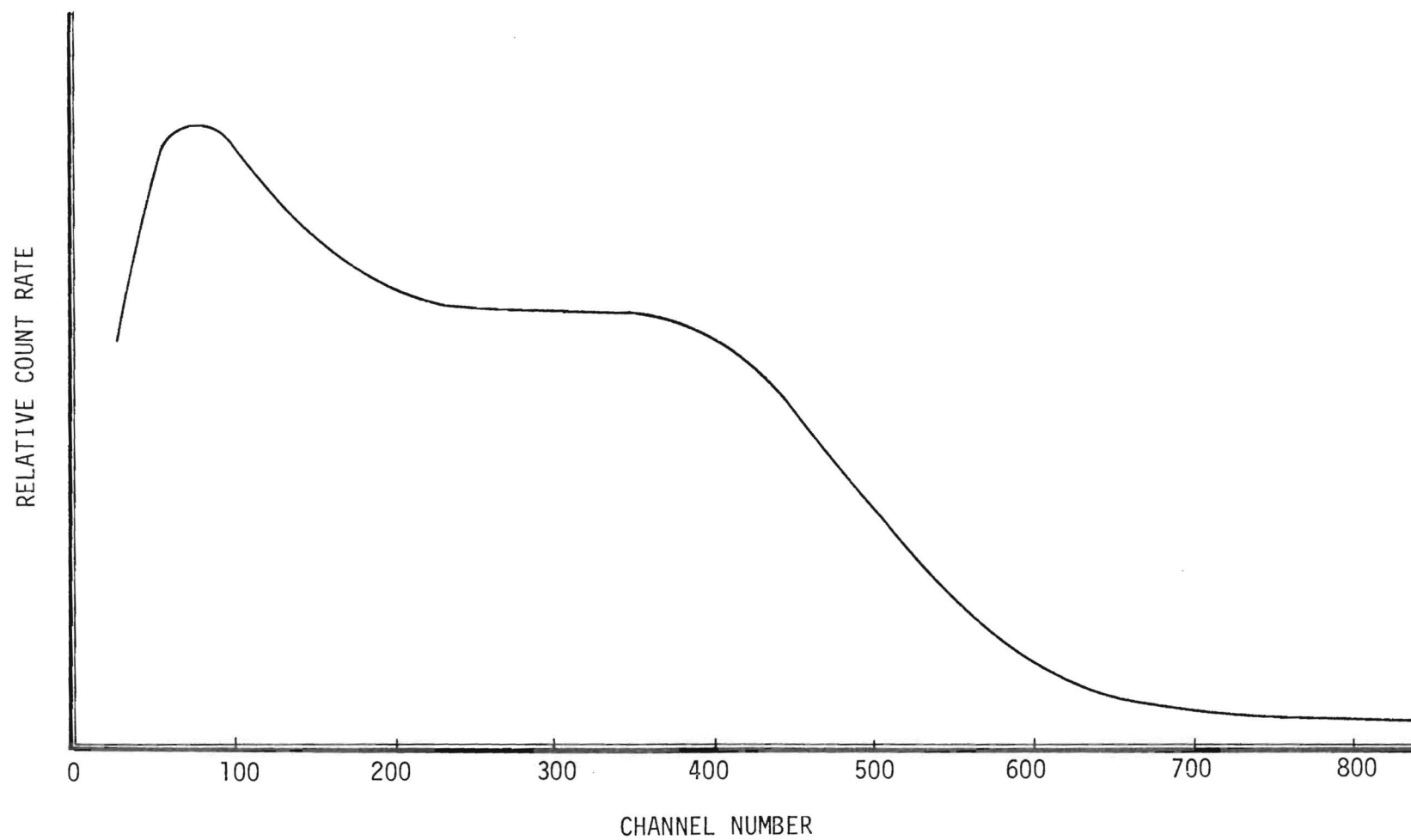FIGURE 7. OCTANE SCINTILLATOR RESPONSE TO 0.84 MEV ^{54}Mn DECAY GAMMA RAY

FIGURE 8. OCTANE SCINTILLATOR RESPONSE TO 0.66 MEV ^{137}Cs DECAY GAMMA RAY

of appropriate sources of low energy gamma rays is being pursued. The complex decay schemes of most radionuclides at low energies prevent the simple interpretation of the pulse height spectra which they produce within the scintillator. An attempt to use the characteristic radiations associated with the irradiation of metal foils with pure beta emitters was also abandonded for similar reasons of complexity. The use of an x-ray machine and crystal monochromator appears to avoid the complexities of previously attempted sources. The investigation of the scintillator response to very low energy gamma rays appears to be feasible by this method.

It is the response of the scintillators to neutrons and protons which is most pertinent to the feasibility investigation. The response of the inner detector liquid scintillator to protons was determined earlier by exposing a test sample to a low energy beam of protons from a van de Graff accelerator. The introduction of low energy protons into the liquid scintillator from an external beam introduces uncertainties by the interaction of the beam with the scintillator window. An experiment is planned which will employ monoenergetic neutrons to produce knock-on protons and hence a continuum of pulses whose energy end point represents the maximum energy transfer. The neutrons will be produced using the pulsed beam Oak Ridge Electron Linear Accelerator (ORELA). The energy selection of neutrons is accomplished electronically by standard time of flight techniques. The advantage of this technique for determining the proton response is that the energy degradation of the neutrons in passing through the cell wall is far less serious than that for protons.

The lithium-6 loading of the outer detector scintillator is about one mole of lithium-6 per kilogram. The lithium-6 is bound in lithium butoxide, a compound which acts solely as a dilutant when added to a scintillator solution. The response of such an octane based scintillator was determined by exposing a one liter volume to a source of thermal neutrons. Figure 9 shows the resulting pulse height spectrum. The electron equivalent energy spectrum was determined by irradiation of the cell with decay gamma rays.

The detection mechanism for neutrons consists of the absorption of a neutron by a lithium-6 nucleus, which subsequently breaks up into a triton and an alpha particle. The Q of this reaction is 4.8 MeV, but the response of the scintillator to the reaction products is much lower than its response to electrons. Consequently, the electron equivalent energy of the peak associated
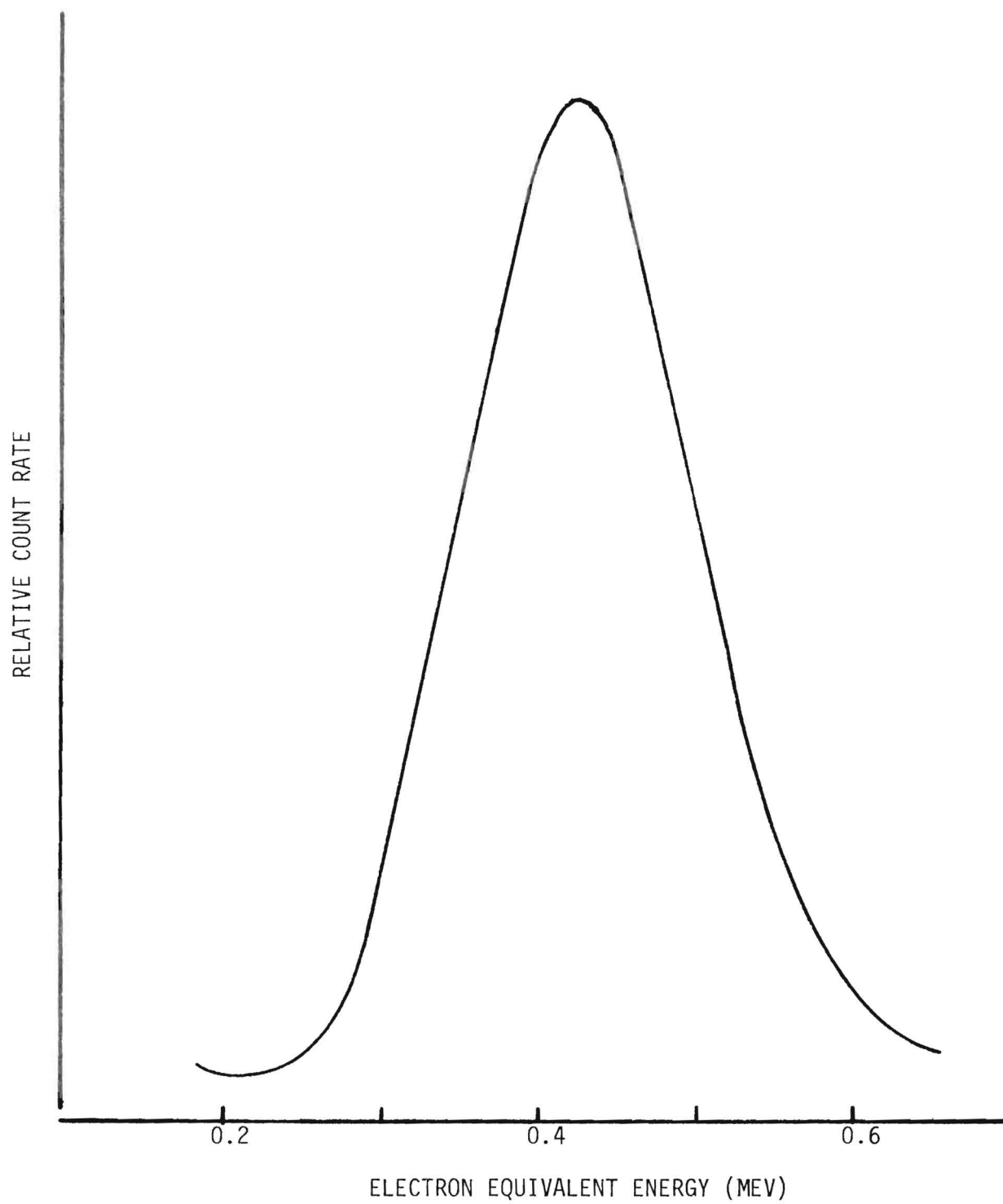
FIGURE 9. ^{6}Li LIQUID SCINTILLATOR RESPONSE TO THERMAL NEUTRONS

with neutron capture is about 0.4 MeV. Neutrons which impinge upon the detector with energies above thermal will typically undergo thermalization collisions prior to being detected. The slow speed of the thermalization process compared to the response time of the scintillator and electronics causes most of this thermalization energy to be lost from the pulse height analysis of the detection reaction. The kinetic energy of neutrons captured before thermalization will be shared by the reaction products, but the low scintillator response to these particles compacts the pulse height spectrum around the high side of the absorption peak.

Shield I Experiments

First Shield Details

Investigation of the background event rates in the prototype detectors required the construction of radiation shields. The first shield (Shield I) is shown in schematic cross section in Figure 10. The asymmetric shape was a consequence of the limited number of lead bricks available. This shape allowed shielding of the first prototype. It also placed the ultimately desired number of lead bricks below the cavity to obviate a total rebuilding of the shield when more bricks became available. The cosmic ray flux consists of hard and soft components. The lead and steel served to shield against the soft component. The borated polyethylene portions consisted of polyethylene bricks which contain 1% boron. They served to thermalize and capture neutrons, both those entering from outside the shield and those created by cosmic rays within the shield itself. The central volume was lined with steel which was covered with electrolytic copper, a material known to be relatively free of radioactivity. The steel imbedded in the lead became the lining for the central cavity in the next shield design. A cosmic ray detector (umbrella) was placed on top of the shield. It consisted of a 60 gallon plexiglass tank filled with a mineral oil based scintillator. Setting the discriminator level below the through peak assured that the umbrella would produce a pulse every time it responded to an ionizing particle capable of penetrating the shield. The rate of events in the through peak was consistent with the known flux of the hard component of the cosmic ray flux, about one particle per square centimeter per minute. A photograph of Shield I taken before the cosmic ray umbrella was installed is shown in Figure 11.

NaI Surveys In Shield I

The investigation of the radiation environment in the laboratory has several motivations. The radiation surveys should allow the identification of sources of interferring background. The knowledge of the gamma ray environment within the shield allows the calculation of the rate of photodisintegration events in the planned experiment. The radiation environment in the laboratory is not exactly that at a reactor, and the accumulation of base line data can aid the extrapolation to the reactor environment.

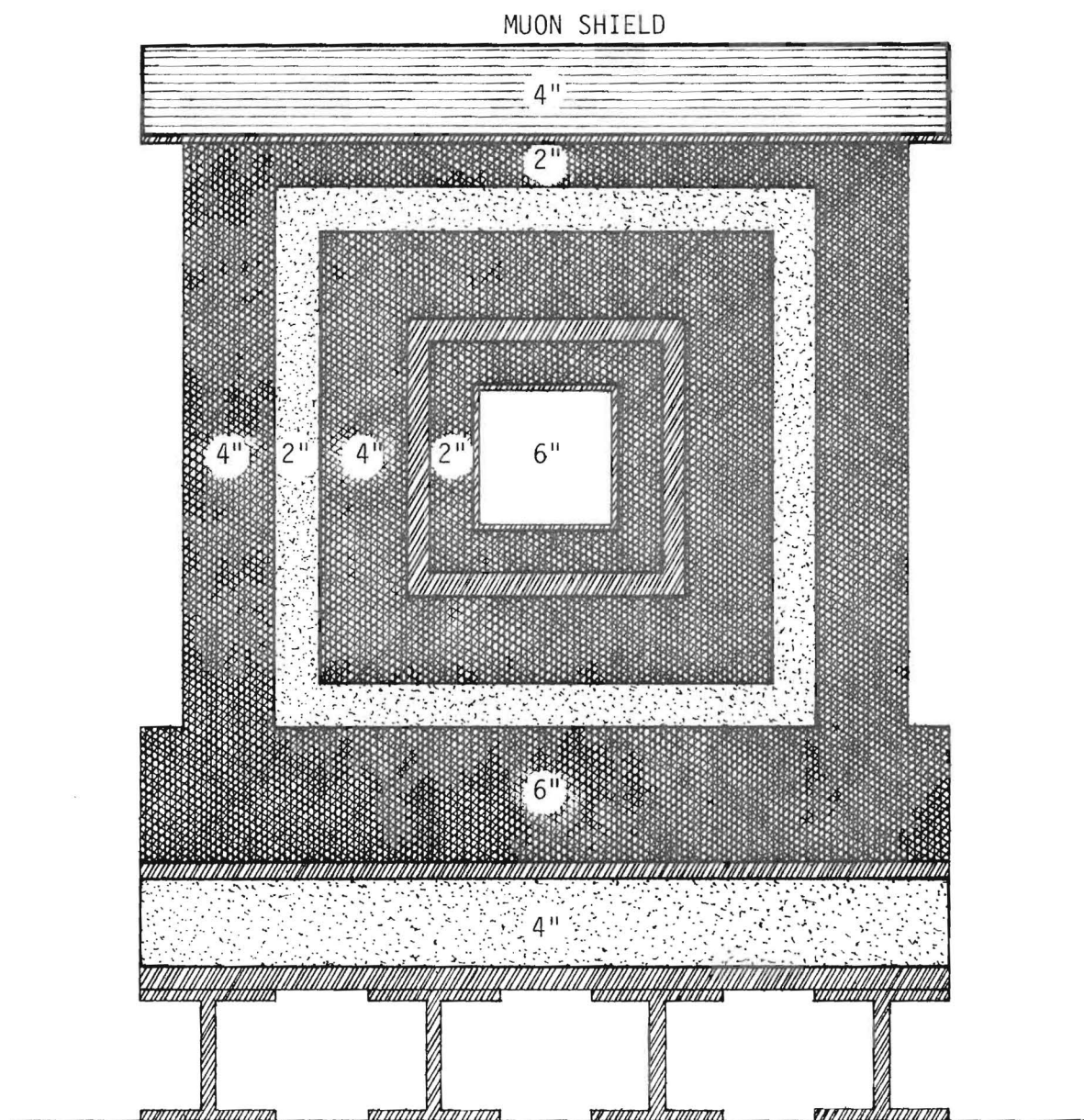|		BOTTOM	SIDES	TOP
▓	LEAD	12"	10"	8"
▨	STEEL	2"	1"	1"
▤	LIQUID SCINTILLATOR	0	0	4"
▦	POLYETHYLENE (BORON LOADED)	6"	2"	2"

MUON SHIELD

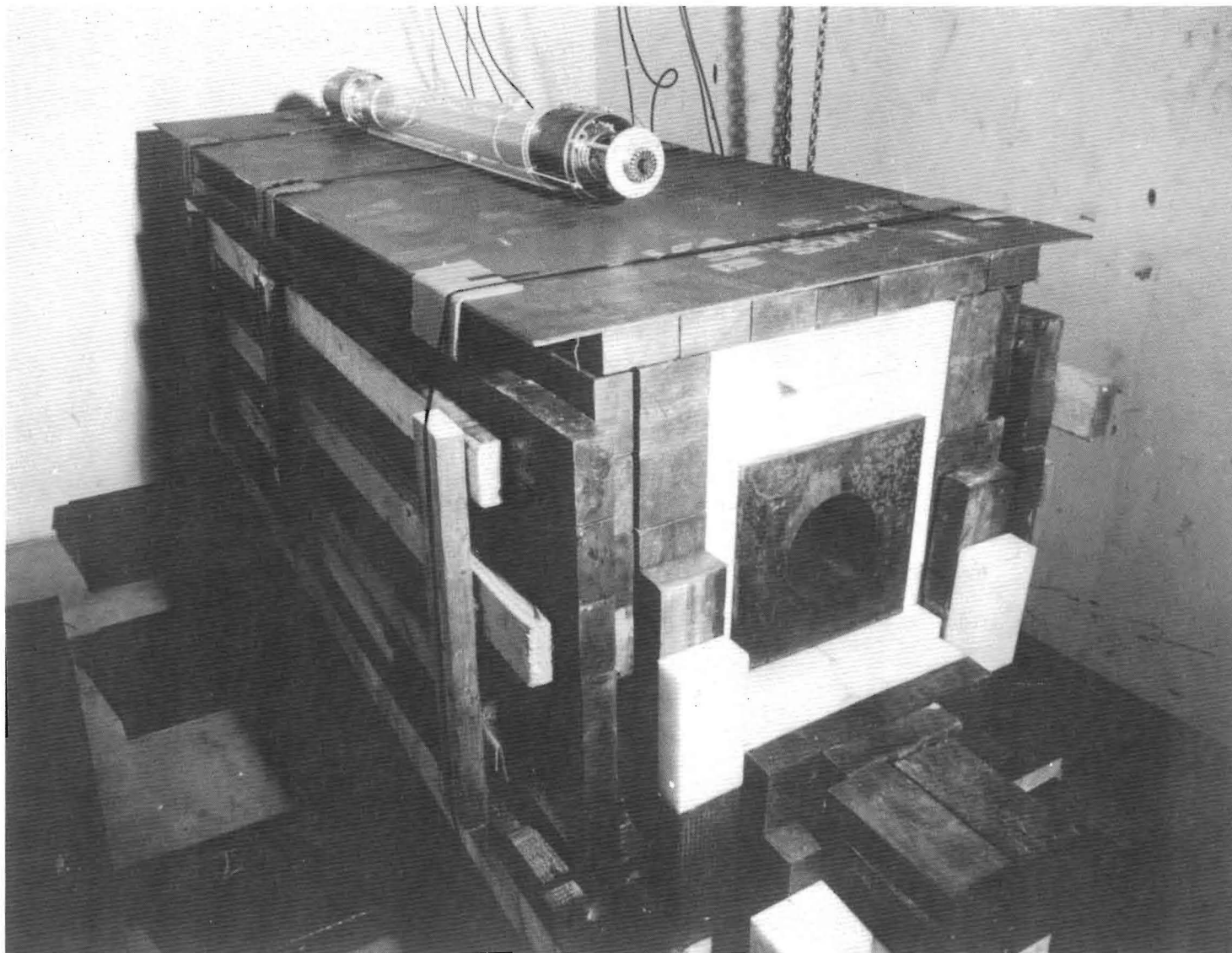

FIGURE 10. SCHEMATIC CROSS SECTION OF SHIELD I

32

FIGURE 11.   PHOTOGRAPH OF PROTOTYPE INNER DETECTOR SITTING ATOP SHIELD I

Within the first shield, these surveys were performed with a 3" x 3" NaI detector. The shield sits within a deep well in the basement of the laboratory building, and a spectrum was accumulated with the detector on the shield supports prior to the construction of Shield I. This spectrum is displayed as the top curve in Figure 12. The structure is associated with identifiable gamma ray decays of common radioactive contaminants. For example, peaks occur which correspond to decays of cobalt-60 (1.17 and 1.33 MeV gamma ray decay energy), potassium-40 (1.46 MeV), and members of the uranium and thorium chains such as thallium-208 (2.62 MeV).

The second curve in Figure 12 displays the spectrum obtained with the detector inside the first shield. The overall reduction of about two orders of magnitude is welcome. Many of the same peaks recur. If the gamma rays were created external to the shield, even the thinnest portion of the shield should have produced a reduction of several more orders of magnitude. The unsurprising conclusion is that the contamination extends to the shield and detector materials.

One possible source of such contamination is the photomultiplier tube; such tubes are in general notoriously "dirty". To test this hypothesis, an eight inch plastic light pipe was inserted between the detector and the photomultiplier tube. The spectrum obtained with the light pipe is shown as the third curve in Figure 12. The peaks associated with gamma ray contamination have been significantly reduced. The reduction in peak heights is consistent with the reduction in the solid angle subtended by the photomultiplier tube.

The remaining continuum does not seem completely explicable as Compton events from these diminished peaks. To demonstrate that much of the continuum is associated with cosmic ray induced events, a spectrum was collected in anti-coincidence with the cosmic ray umbrella. The lowest curve in Figure 12 illustrates this spectrum. A general reduction of the spectrum is observed. The gamma ray peaks re-emerge from the continuum since the rate of decay of radioactive contaminants should be unrelated to cosmic rays.

These results bear upon the proposed experiment in several ways. One expects cosmic ray anticoincidence to reduce the background for the experiment. Recommending the use of light pipes is redundant, for their presence is desired for their salubrious effect upon the uniformity of the detector spatial response. Techniques for selection of materials for low radioactive contamination have been developed.
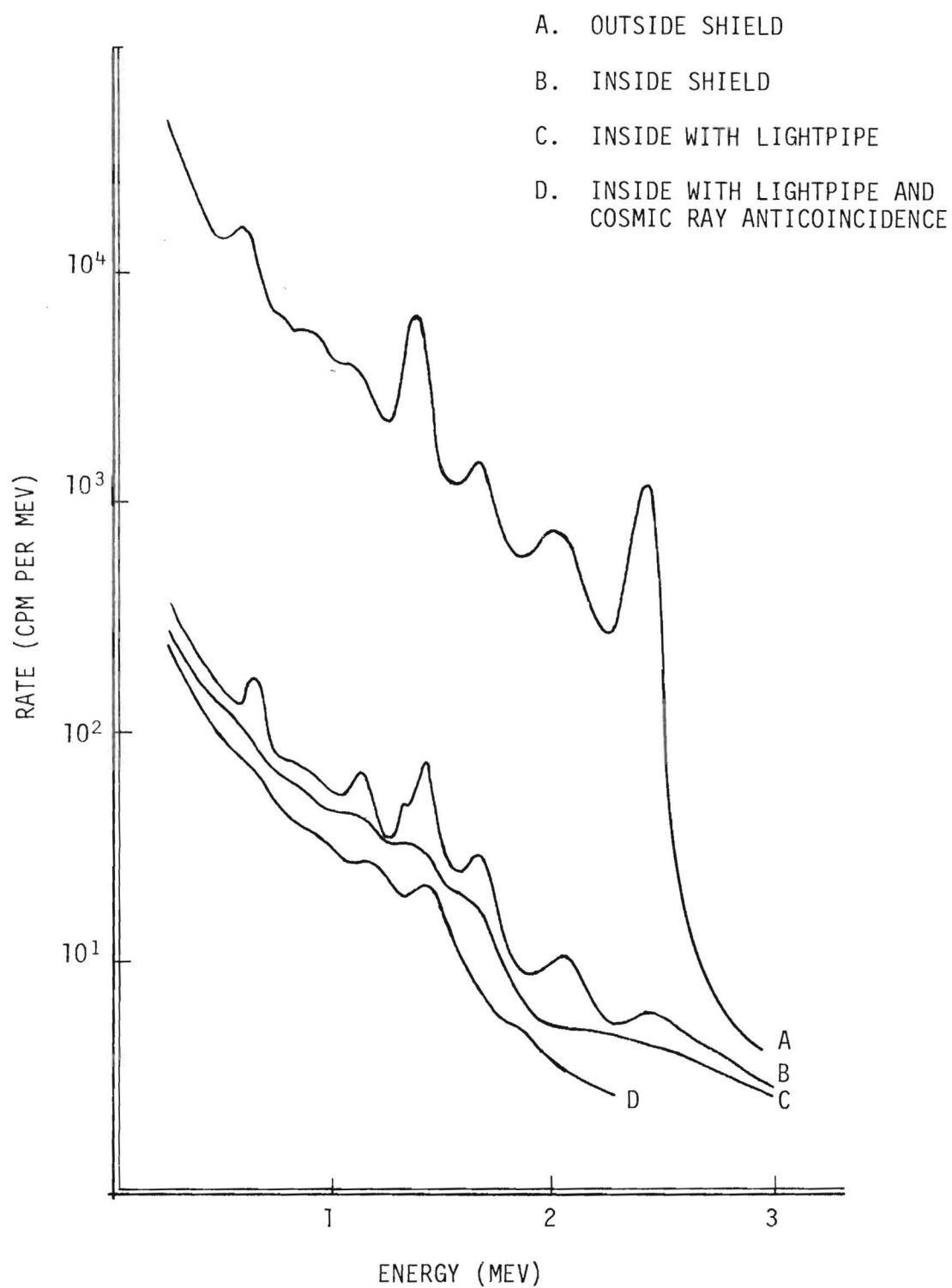
A. OUTSIDE SHIELD

B. INSIDE SHIELD

C. INSIDE WITH LIGHTPIPE

D. INSIDE WITH LIGHTPIPE AND
   COSMIC RAY ANTICOINCIDENCE

FIGURE 12. NaI SURVEYS OF SHIELD I

35

Time Correlation In Adjacent Detectors

The signature for the antineutrino deuteron disintegration experiment consists of two pulses from separate detectors which occur within a 33 microsecond coincidence window. The background consists of all events which cause a similar signature, but which are not caused by protons and neutrons resulting from the antineutrino disintegration of a deuteron.

There exists the possibility that many of the coincidence events which occur in two closely adjacent detectors will have a time correlation signature which will allow their rejection as background. For example, the scattering of a gamma ray from one detector to another can only occur in very short times if the detectors are closely adjacent, as they must be in each of the experimental modules. The measurement of this effect in the prototype of the dual concentric module is underway but not yet completed. However, many of the features of the correlation should be present for any two closely adjacent detectors, such as two NaI detectors in close proximity.

To examine this effect, two adjacent 3" x 3" NaI detectors were placed in the shield, and the delay between the pulse occuring in one detector and the next pulse from the other detector measured. The spectrum of such delays is shown in Figure 13. The peak falls to half its maximum well within 50 nanoseconds. The ratio of the integral of the peak within 400 nanoseconds of zero delay to that from 400 nanoseconds to 33 microseconds is about 25 to one. Consequently, one distinguishing feature of the correlated background in two closely adjacent detectors is that it occurs in short times (tens of nanoseconds), at least for the radiations to which a NaI detector is sensitive.

Central Detector Prototype

The presently conceived experiment consists of six identical modules, each with a central cylindrical detector surrounded by another cylindrical sheath detector. The inner detector serves both as target and as the proton detector. The outer one detects the neutrons.

A prototype of the central detector was constructed. A photograph of the prototype is displayed in Figure 14. More detailed features are shown in the upper drawing in Figure 23. The construction material was 1/4 inch plexiglass. The central volume was filled with the previously selected optimum octane based scintillator and the two end volumes with pure octane.
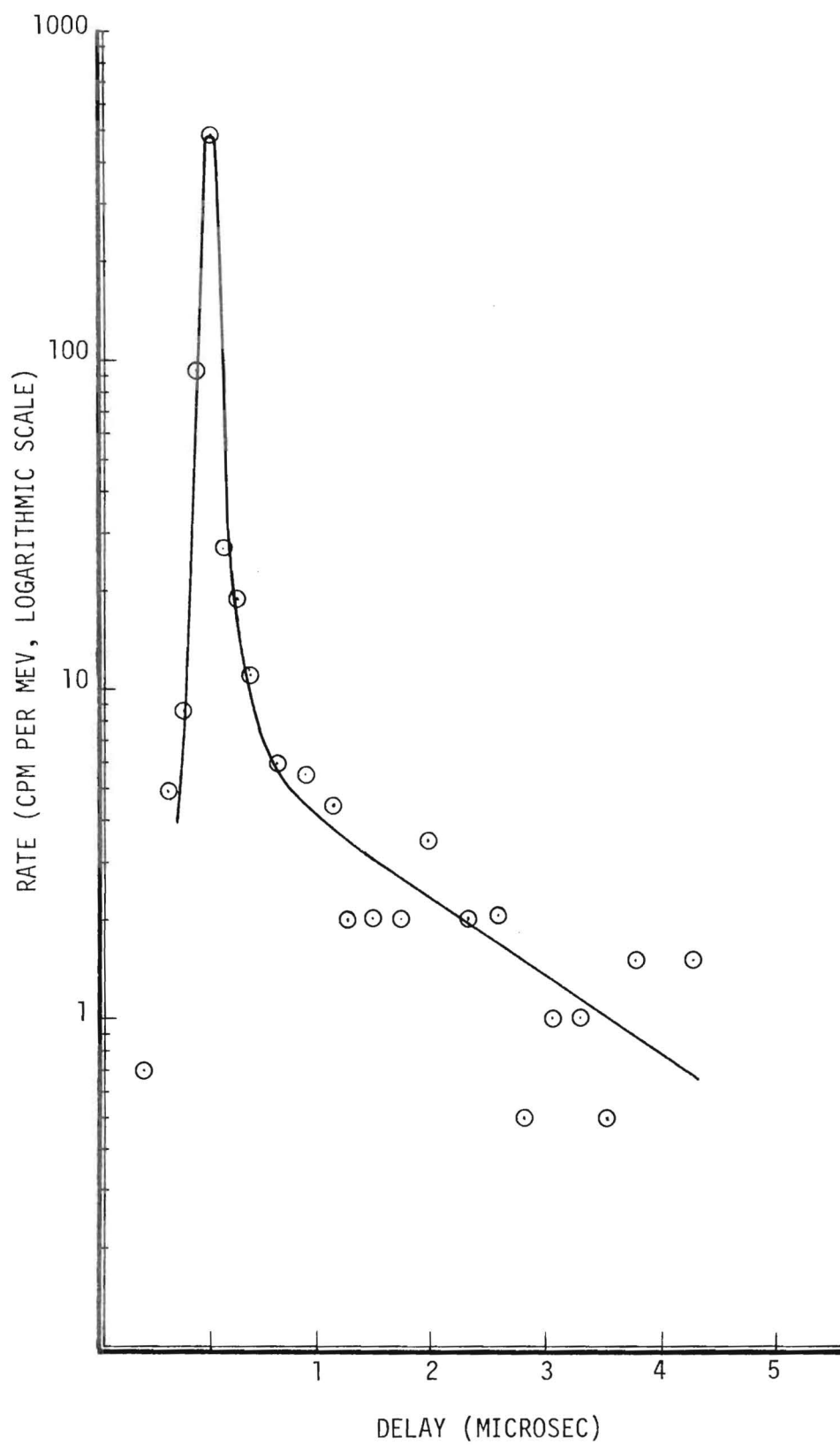
FIGURE 13. SPECTRUM OF TIME DELAYS BETWEEN COINCIDENT PULSES
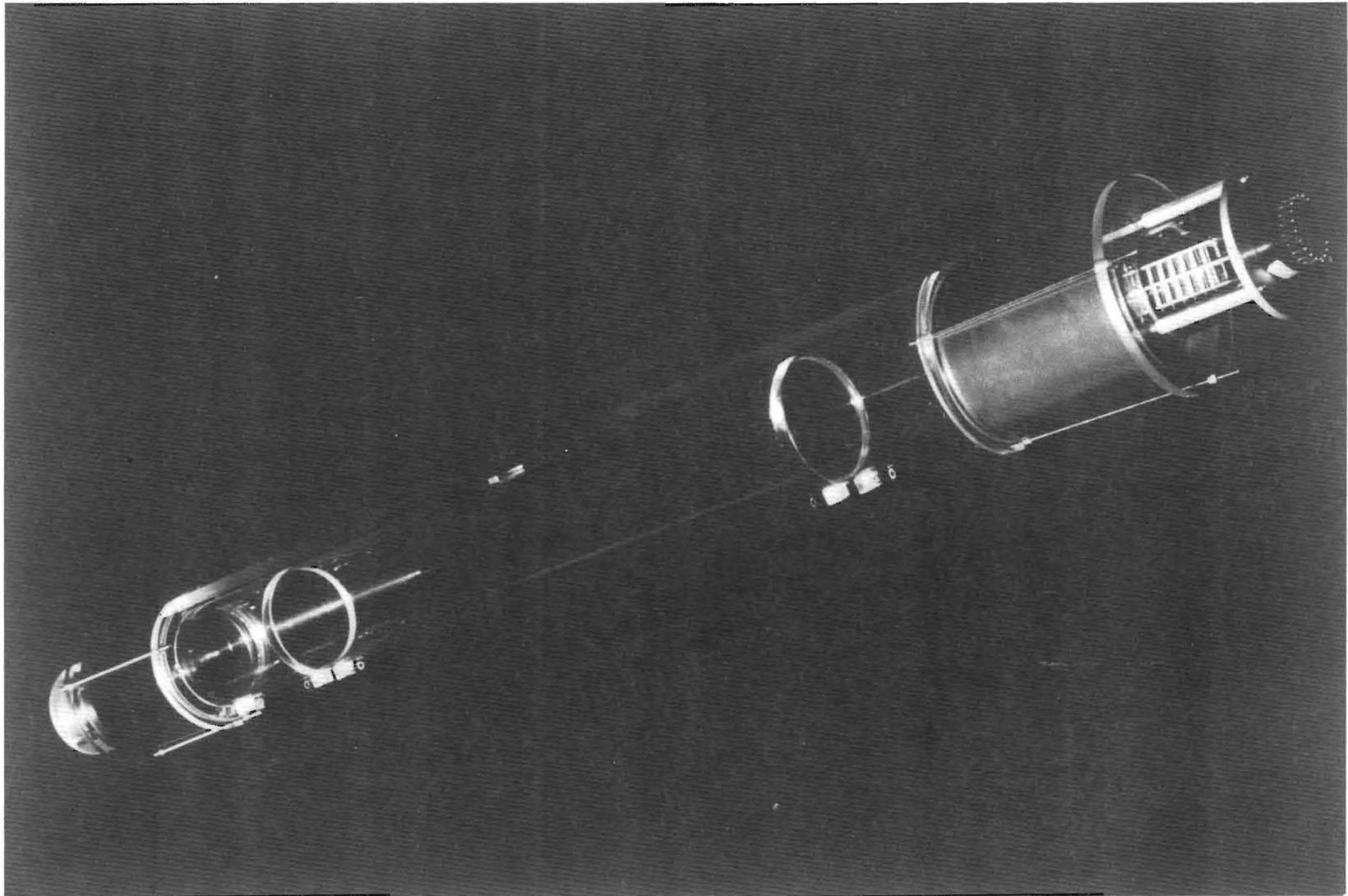FROM TWO ADJACENT NaI DETECTORS

37

FIGURE 14. PHOTOGRAPH OF PROTOTYPE INNER DETECTOR

The use of two photomultiplier tubes operated in coincidence reduces the low energy background count rate from photomultiplier dark current and electronic noise. Further reduction is accomplished by the use of low dark current photomultiplier tubes. The Amperex XP1040 is suited to this application. In addition to its fast timing characteristics, it is inherently low in dark current. A comparison of the dark current spectra from all the XP1040 photomultiplier tubes available in the laboratory was obtained. Each tube was energy calibrated by coupling it to a 2" x 2" NaI crystal, and adjusting the electronic gain so that the photopeak of a cesium-137 decay gamma ray fell in a given channel in the multichannel analyzer. The detector was removed, and the pulse height spectrum collected. To assure that the conditions were not altered between tests, a second XP1040 remained in the light tight box and its spectrum collected concurrently during each of the tests. The two tubes with the lowest dark current spectrum were selected for mounting on the prototype.

Central Detector Spectra

The central detector prototype was inserted in the first shield (See Figure 15), and energy calibrated. Pulse height spectra were collected with and without a 4 microsecond wide cosmic ray umbrella gate. The results are displayed in Figure 16.

The most surprising result of these spectra is the structure, a broad peak about 0.4 MeV. The coincidence spectrum shows it is in coincidence with the cosmic ray umbrella. It is not the fabled through peak for its energy is much too low. The anticoincidence spectrum is more like the monotonically decreasing spectrum one might expect to observe.

The source of the peak is something of a puzzle. Its shape is inconsistent with an origin from gamma rays. (Compare, for example, the cesium-137 calibration spectrum of Figure 8.) Uncharged particles such as neutrons could produce pulses within the detector by knockon processes, but to produce a peak the incident particles would have to be sharply defined in energy, which seems unlikely. One is left with the conclusion that some charged particle in coincidence with the cosmic ray umbrella produces the peak in the detector with an electron equivalent energy of 0.4 MeV. The differing response of the NaI detector to charged particles makes it difficult to attempt to find this peak in that spectrum. The peaks in the NaI spectra have acceptable explanations
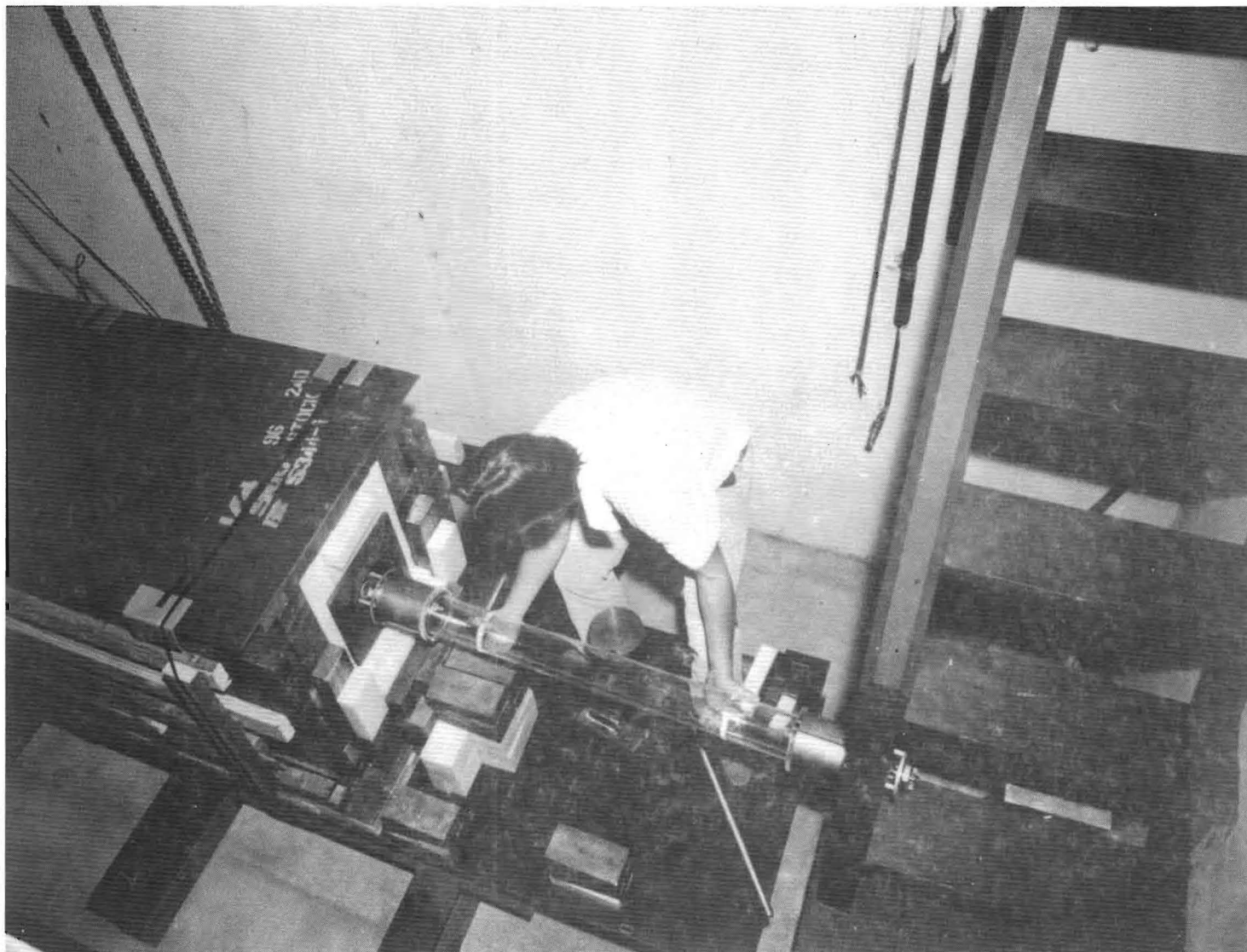
FIGURE 15. PHOTOGRAPH OF INSERTING PROTOTYPE INNER DETECTOR INTO SHIELD I

A. INSIDE SHIELD

B. INSIDE WITH COSMIC RAY COINCIDENCE

C. INSIDE WITH COSMIC RAY ANTICOINCIDENCE

RATE (CPM PER MEV)

3000

2000

1000

A

B

C

500

ELECTRON EQUIVALENT ENERGY (KEV)
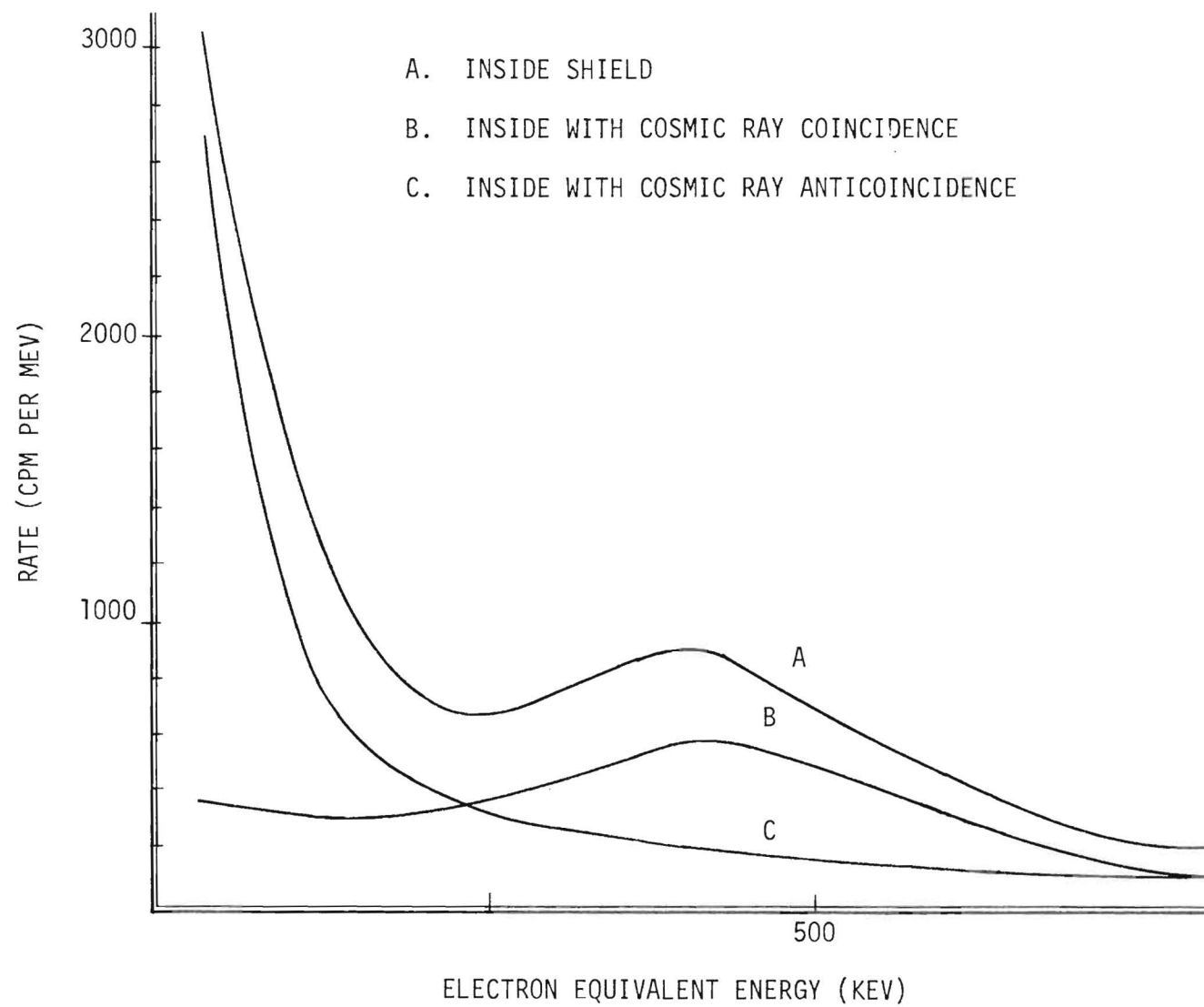
FIGURE 16.   PULSE HEIGHT SPECTRA OF BACKGROUND IN INNER DETECTOR PROTOTYPE

in their association with decay gamma rays. This peak is present in the lithium loaded scintillator data. It is so close in energy to the neutron peak that it is not resolved.

At any rate, it disappears in the anticoincidence spectrum. From these data, one can calculate the rate of events in the proton window. With no gate, the rate is 266 ± 3 counts per minute. In anticoincidence it is 214.7 ± 0.7 counts per minute.

Knowing that the neutron peak would appear around 0.4 MeV if the neutron scintillator were lithium-6 loaded, one can calculate the rates in the window. These should correspond to background rates in the neutron detector without the presence of neutrons. The rate with no gate is 234 ± 3 counts per minute, and 78.6 ± 0.4 counts per minute in anticoincidence.

Shield II Experiments

Second Shield Details

The acquisition of 500 more lead bricks and nineteen sheets of one percent borated polyethylene allowed the construction of a new shield (Shield II) capable of shielding the entire two detector module and photomultiplier tubes. Shield II is shown schematically in Figure 17.

There are now ten inches of lead in all directions from the sensitive volume of the detectors. For neutron shielding, two complete two inch thick shells of borated polyethylene surround the central volume. The central volume is now lined with one-half inch of steel, coated with electrolytic copper.

The new cosmic ray umbrella consists of three tanks of mineral oil scintillator, arranged so as to completely shield the central volume on two sides and the top. These tanks were calibrated as before, namely, the through peak was obtained in each and discriminator levels set well below the peak. A pulse from any of these tanks is sufficient to qualify as an output from the umbrella. Details of the structure are shown in Figure 18.

Neutron Source Probes

The properties of this shield were investigated by placing a californium-252 source of fission neutrons at various points around the shield. Both neutron and gamma ray fluxes within the shield were measured. The presence of neutron associated gamma rays within the shield is expected from the gamma ray decay of neutron capture products. These tests allow a determination of the ability of the present shield configuration to shield the experimental modules from the radiation produced by a reactor.

The neutron detector used was a LiI(Eu) detector, the neutron detection mechanism of which consists of the same reaction which is used in the outer detector of the experimental module. The results of this survey are shown in Table IV.

The parameter R is defined as the ratio of observed counts to the expected rate if the source were a simple point emitting neutrons isotropically. The observed values of R indicate that the shield attenuates neutrons by about three orders of magnitude. A comparison of the third and fourth values of R indicates the effect of the mineral oil as a passive neutron shield. The actual

43

MUON SHIELDS

5"

4"   4"

2" 6" 2" 4"   10.75"

4"

LEAD

STEEL
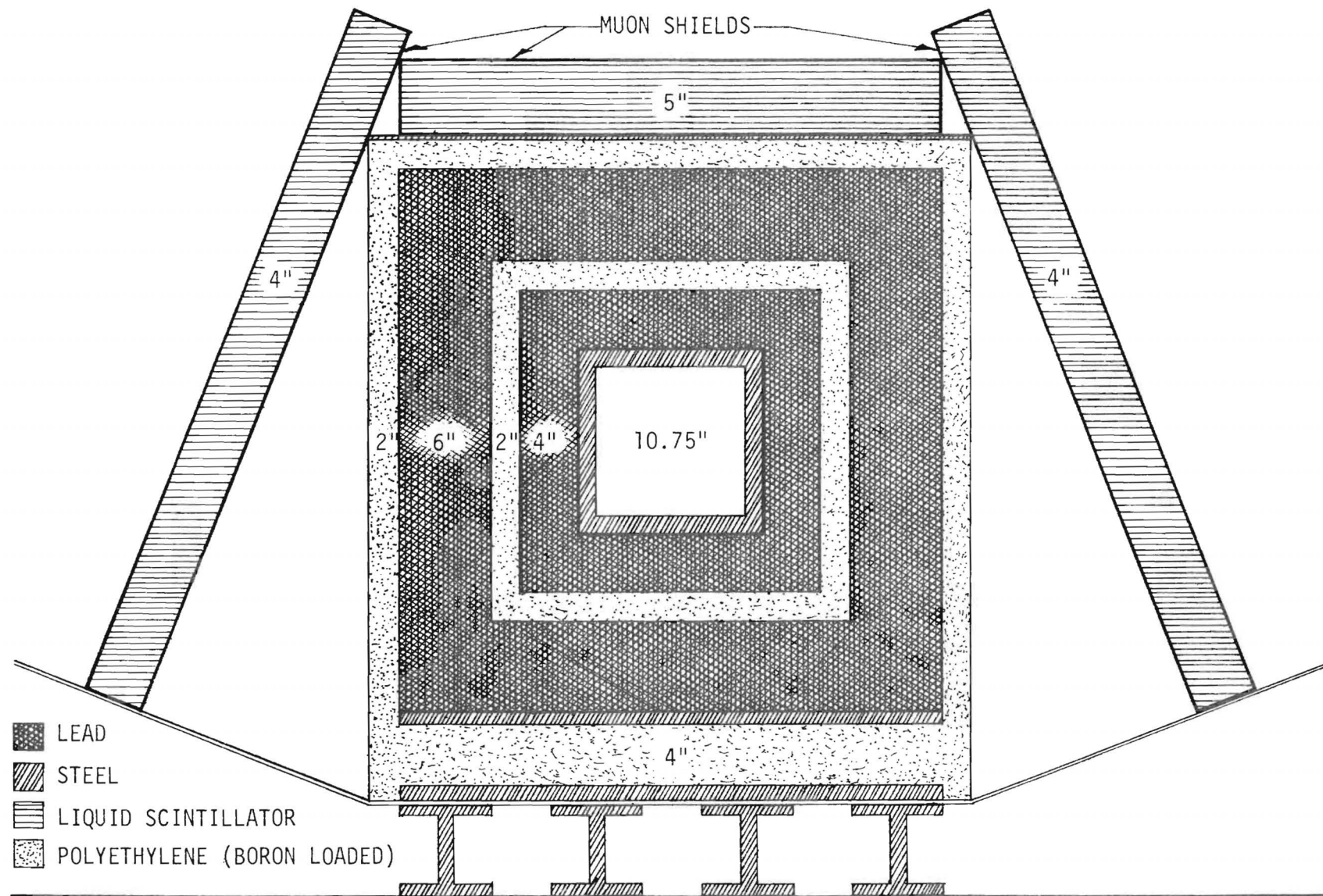
LIQUID SCINTILLATOR

POLYETHYLENE (BORON LOADED)

44

FIGURE 17. SCHEMATIC CROSS SECTION OF SHIELD II

FIGURE 18. PHOTOGRAPH OF SHIELD II UNDER CONSTRUCTION

rate of the observed neutron counts is not pertinent, for the flux of neutrons from the source at the shield is considerably in excess of that present in biologically safe areas near reactors.

The pulse height spectrum from a NaI detector within the shield due to a californium-252 neutron source outside the shield is shown in Figure 19. The peaks in the gamma ray spectrum are apparently associated with neutron activation gamma rays. For example, there is a peak around 0.5 MeV which may be identified as resulting from the absorption of a neutron by the boron in the borated polyethylene. The rates of these peaks are shown in the table, ratioed to the neutron rate with the source at that location.

Besides contributing to the background within the energy windows in the inner and outer detectors, neutron activation gamma rays can contribute to the photodisintegration rate, and thus mimic the signal. The absorption of a neutron in lead and iron leads to many decay gamma rays which are sufficiently energetic to cause photodisintegration. The rates of gamma rays from the deuteron breakup threshold, 2.2 MeV, to the upper end of the gamma rays from neutron activation in the shield materials, 8.0 MeV, were calculated and are also shown in Table IV as ratios to the neutron rates.

The spread of these ratios about the average is consistant with the statistical uncertainties of the ratios. The constancy of these values emphasizes the relationship between these gamma rays and the neutron flux within the shield.

TABLE IV. NEUTRON SOURCE PROBE OF SHIELD

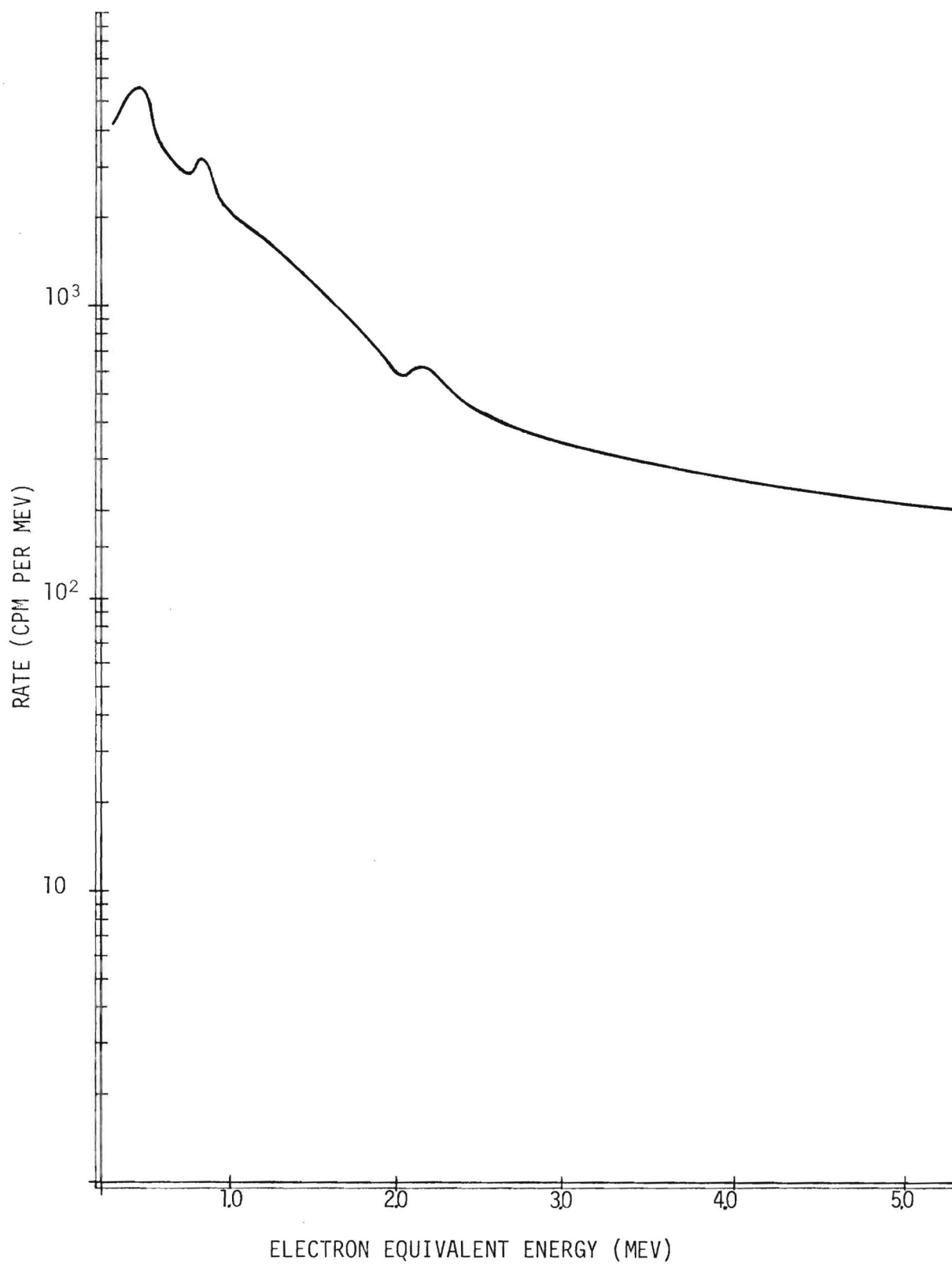| Location of Source | R | Gamma Ray Energy in MeV | | | |
		0.5	0.85	2.2	2.2 to 8.0
Shield End	0.0052	0.41	0.035	0.023	1.12
Shield Top	0.00028	0.11	0.069	0.027	1.74
Shield Side	0.00086	0.054	0.052	0.031	1.43
Between Side Umbrella and Shield	0.0030	0.053	0.047	0.034	1.42
Irradiating Shield From Oblique Angle	0.0012				
AVERAGES:		0.146	0.049	0.031	1.40

46

FIGURE 19.   NEUTRON INDUCED NaI SPECTRUM WITHIN SHIELD II

The shielding of the inner volume from reactor produced gamma rays is straightforward. Given reasonable care to assure that there are no blanks in the shield, the gamma ray flux originating outside the shield can readily be reduced to acceptable values. The reduction of reactor associated neutron fluxes to acceptable levels is also possible, considering the experience of previous workers. Given a knowledge of the reactor associated neutron and gamma ray fluxes at the experimental site, the data collected here can aid the final design of the shield for the planned experiment.

NaI Surveys In Shield II

Upon completion of the second shield, some NaI surveys were performed to confirm that the radiation environment of the shielded volume was not degraded. The data were obtained with the same 3" x 3" NaI detector used previously, with the eight inch light pipe and a different photomultiplier tube. The results of these surveys are shown in Figure 20.

The top spectrum was obtained with the detector located outside the shield well on the laboratory floor. Since the shield construction occupied the well, it was not possible to place the detector in the same location as that for which the previous unshielded spectrum was obtained. Comparison of the present spectrum with the top one in Figure 12 demonstrates that the two are quite similar.

The second spectrum in Figure 20 was collected with the detector inside the shield. The experimental conditions are similar to those of the third curve of Figure 12. The present spectrum is generally lower, which demonstrates that the environment within Shield II is a little "cleaner". Both the peaks and the continuum are lower than before. The lowered continuum accentuates the gamma ray peaks. Detailed analysis indicates that the Shield II peak rates are somewhat lower than the peak rates of the first shield survey, which suggests that the materials surrounding the shielded volume are less contaminated.
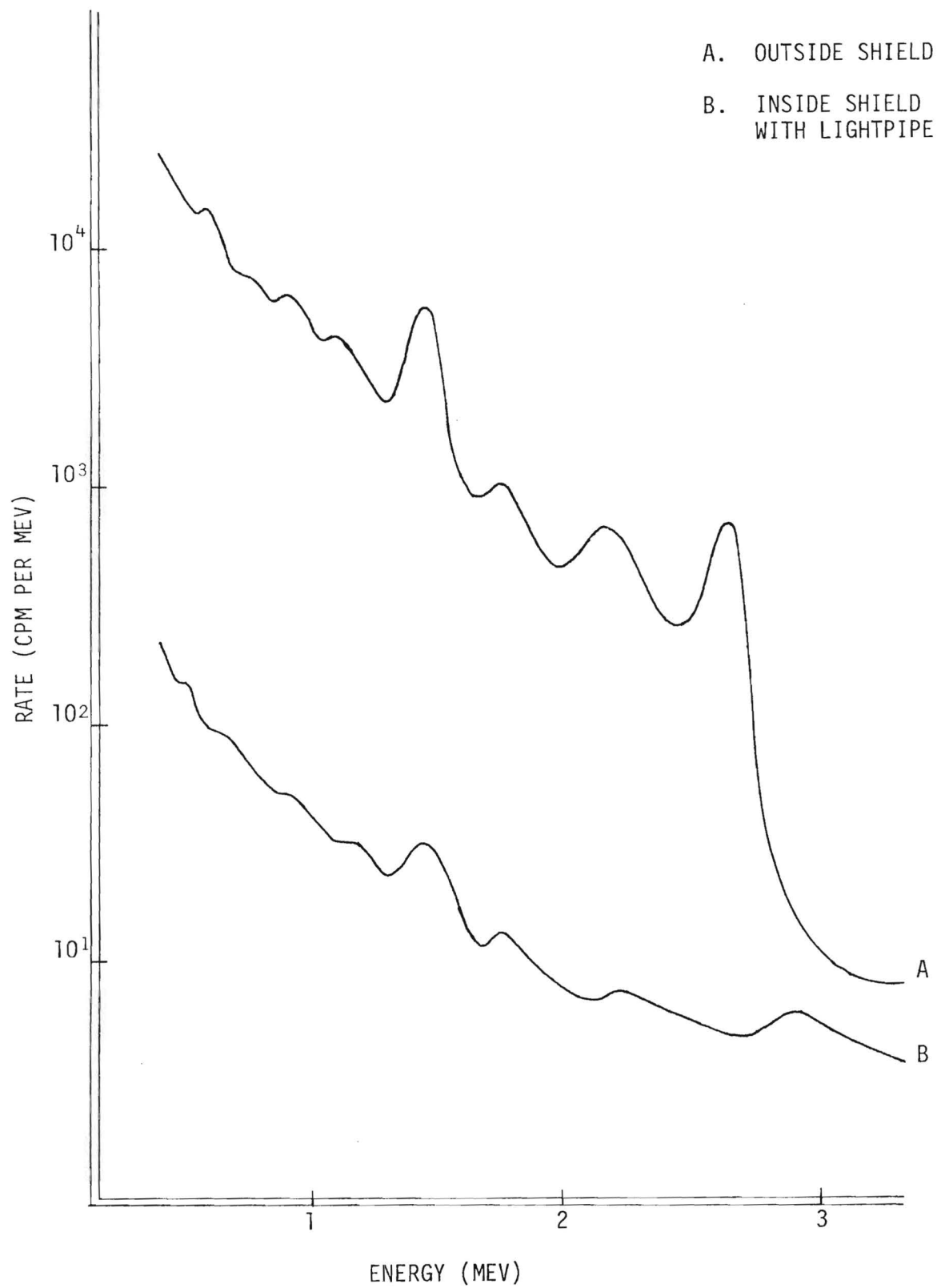
A. OUTSIDE SHIELD

B. INSIDE SHIELD
WITH LIGHTPIPE

FIGURE 20. NaI SURVEYS OF SHIELD II

49

Ambient Neutron Studies

The presence of ambient neutrons can cause background events in the detector modules, both by absorption in the neutron detector and by inelastic collisions in either detector. A survey of the neutron fluxes in the laboratory can provide a measure of the seriousness of these sources of background.

Two detectors were used in making these surveys, a lithium-6 loaded solid LiI crystal and a one liter lithium-6 loaded liquid scintillator. Both depend upon the detection of the reaction products following the absorption of a neutron by lithium-6. Both detectors were calibrated by exposure to a californium-252 neutron source of known activity.

Several measurements with the LiI detector, both bare and surrounded by various amounts of paraffin, were unable to observe a neutron flux outside the shield. The lowest upper limit which was determined was about 0.01 neutrons per square centimeter per second. The neutron flux near the surface of the earth is known to be low, 0.002 neutrons per square centimeter per second (cf Hendrix and Edge PHYS. REV. 145, p. 1023, 1966). The LiI detector is sensitive to gamma rays, and the high flux of gamma rays prevents the observation of the low fluxes of neutrons.

Within the shield, the gamma ray flux is reduced by about two orders of magnitude, so lower fluxes are observable. The two detectors yielded rates which are comparable to thermal fluxes of about 0.001 neutrons per square centimeter per second.

Data accumulated with the one liter cell of lithium-6 loaded scintillator may be used to estimate the rate of events in the lithium-6 loaded outer detector of the detector module. The cell, observed by two photomultiplier tubes operated in coincidence, was inserted in the shield and calibrated in electron equivalent energies using gamma ray sources, and the spectrum from californium-252 neutrons obtained. This spectrum is displayed in Figure 21.

The pulse height spectrum within the shield was observed both with and without a 5 microsecond wide anticoincidence cosmic ray umbrella gate. The results are displayed in Figure 22. The shoulder in the low energy portion of these spectra is associated with the neutrons, for it occurs at the appropriate energy. The peak which occurred in the inner detector prototype (Figure 16) must also contribute to the peak in this present spectrum.
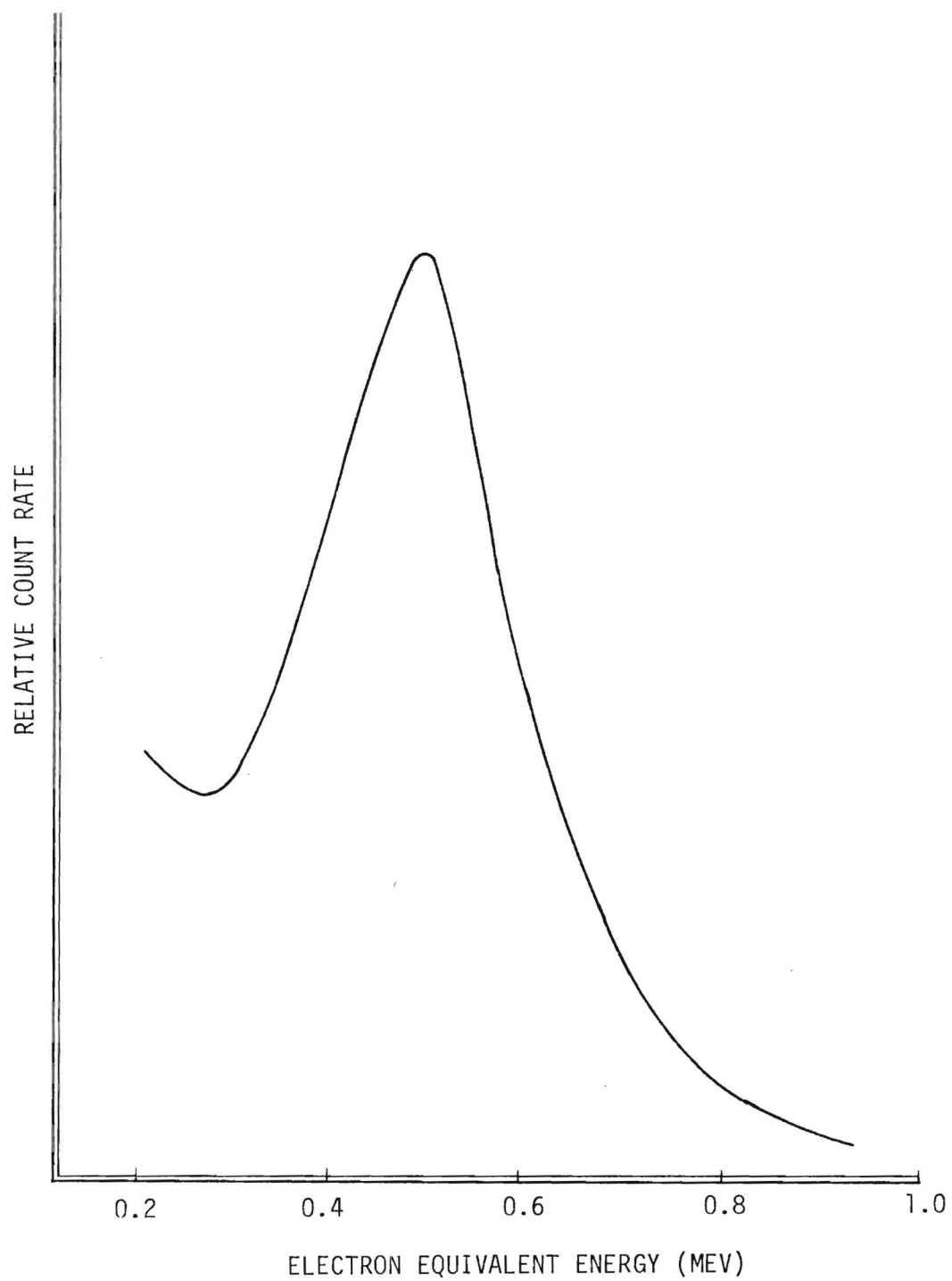
FIGURE 21. ⁶LI LIQUID SCINTILLATOR RESPONSE TO ²⁵²CF NEUTRONS

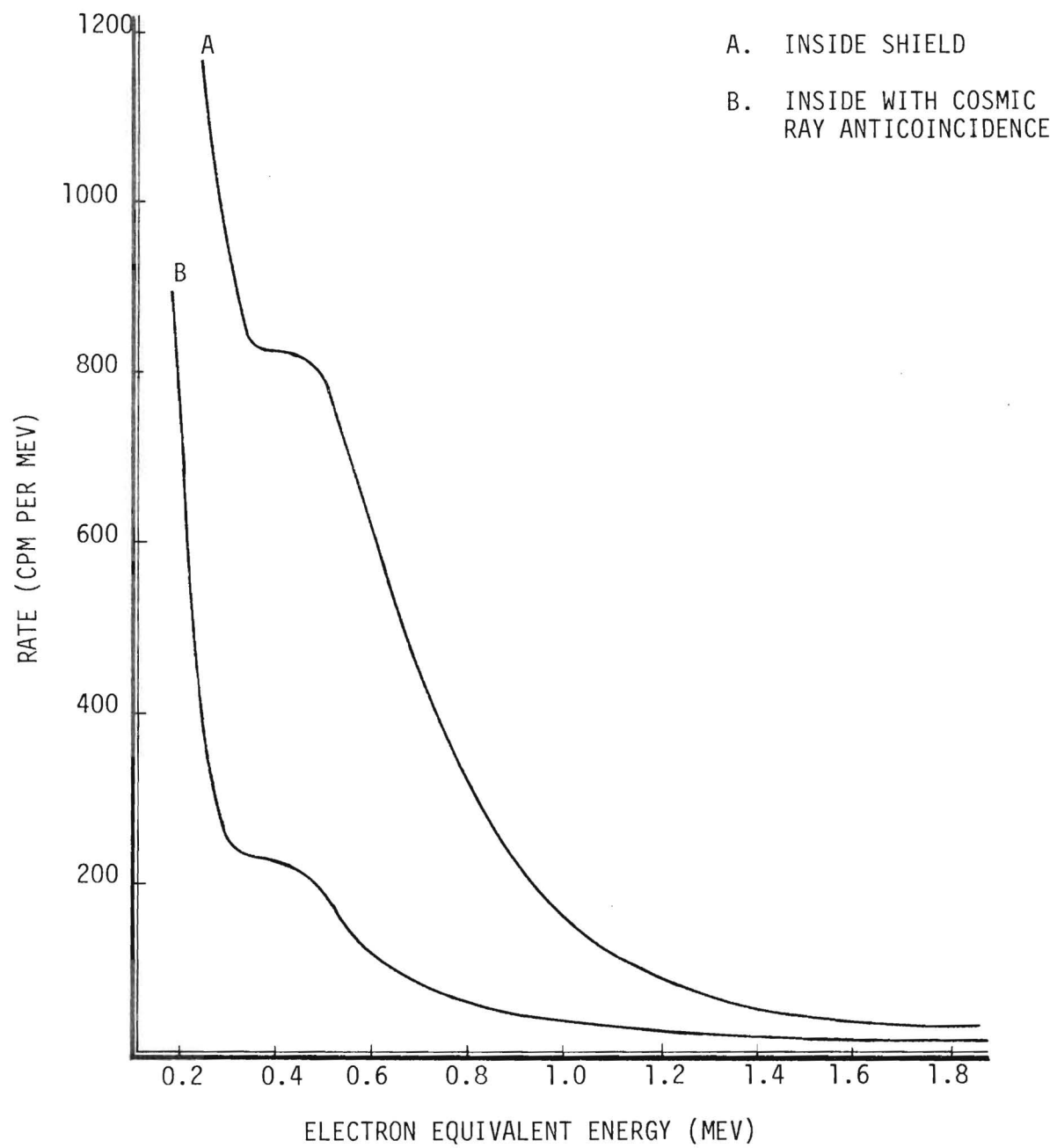FIGURE 21. ^{6}LI LIQUID SCINTILLATOR RESPONSE TO ^{252}CF NEUTRONS

51

FIGURE 22.   ⁶LI LIQUID SCINTILLATOR SPECTRA IN SHIELD II

The reduction of the peak height caused by the anticoincidence gate implies that the neutrons are created in the shield by cosmic ray interactions. A long time width for the anticoincidence gate is indicated for removing the effects of the neutrons, for flight times of neutrons through the shield are slower than those of the swift cosmic rays. The five microsecond wide gate accomplished a factor of five reduction in the peak rate. A gate width of 500 microseconds was required to reduce the neutron peak rate by another factor of about five.

From these spectra, the singles rates within the neutron window of the lithium-6 loaded scintillator can be determined. The rate without anticoincidence is 323.2 ± 0.6 cpm, and with a five microsecond wide anticoincidence gate is 77.9 ± 0.2 cpm. The neutron peak rates, i.e., window minus exponential background, are 36.0 ± 0.7 cpm and 6.0 ± 0.8 cpm without and with the five microsecond wide anticoincidence gate, respectively.

These values were quite curious. The background rates, total rate minus peak rate, are 287 cpm without gate and 71 cpm with gate. These should be comparable to the rates obtained in the inner detector prototype in the neutron energy window: 40 cpm and 20 cpm, respectively, when scaled to one liter.

The appearance of higher background in the lithium-6 loaded scintillator was unpleasant. The source of these events was shown to be the glass cell used to contain the lithium-6 loaded scintillator. Most glass is rather heavily contaminated with radioactive materials.

To investigate this, the optimum non-lithium loaded scintillator was substituted for the lithium-6 loaded scintillator in the same glass cell, and spectra collected. Comparable background rates were observed.

Prototype of Experimental Module

To examine the characteristics of a complete, two detector module, a prototype has been constructed. The details of its dimensions and construction are shown in Figure 23. The inner cell is the same as the inner detector prototype, and the outer, neutron detector portion has been added. Two Amperex XP2041 photomultiplier tubes are mounted on the inner detector light pipes. Two nine inch diameter Amperex 57AVP photomultiplier tubes are mounted on the light pipes at the ends of the module. The outer light pipes consist of cylindrical volumes filled with pure nonscintillating solvent, capped by a solid piece of plexiglass which directs the light to the photocathode of the photomultiplier tube. Access to the inner photomultiplier tubes is available through slots milled in the solid light pipes on each end. Details of the light pipes for the outer detector are shown in Figure 24.

The module has been inserted into the shield and some preliminary data have been obtained concerning the time relationship between pulses in the two detectors. The experimental scheme causes a pulse from the inner detector which is coincident in both photomultiplier tubes which view the scintillator and which is within the proton energy window to start the time to amplitude converter (TAC). An outer detector pulse which is coincident in both photomultiplier tubes which view that scintillator and which is within the neutron energy window will stop the TAC. A schematic of this arrangement is shown in Figure 25. The results of a time delay spectrum collected in this manner are displayed as the top curve in Figure 26. Neither the cosmic ray anticoincidence nor the prompt rejection criteria were applied for this first experiment. The prompt dwarfs other portions of the spectrum, just as in the similar NaI detector experiment.

The effects of the rejection of prompt coincidence events and the cosmic ray anticoincidence upon the time relationship has been investigated with the same arrangement shown schematically in Figure 25. Each requirement can be applied individually. The lower curve of Figure 26 shows the effect upon the prompt peak of the rejection of prompt coincidence events (those within 100 nanoseconds.) The prompt peak is reduced by a factor of about 20.

54

5" PM TUBE

9" PM TUBE

6½"   26"   6½"

4"   19-3/4"   26"   19-3/4"   4"
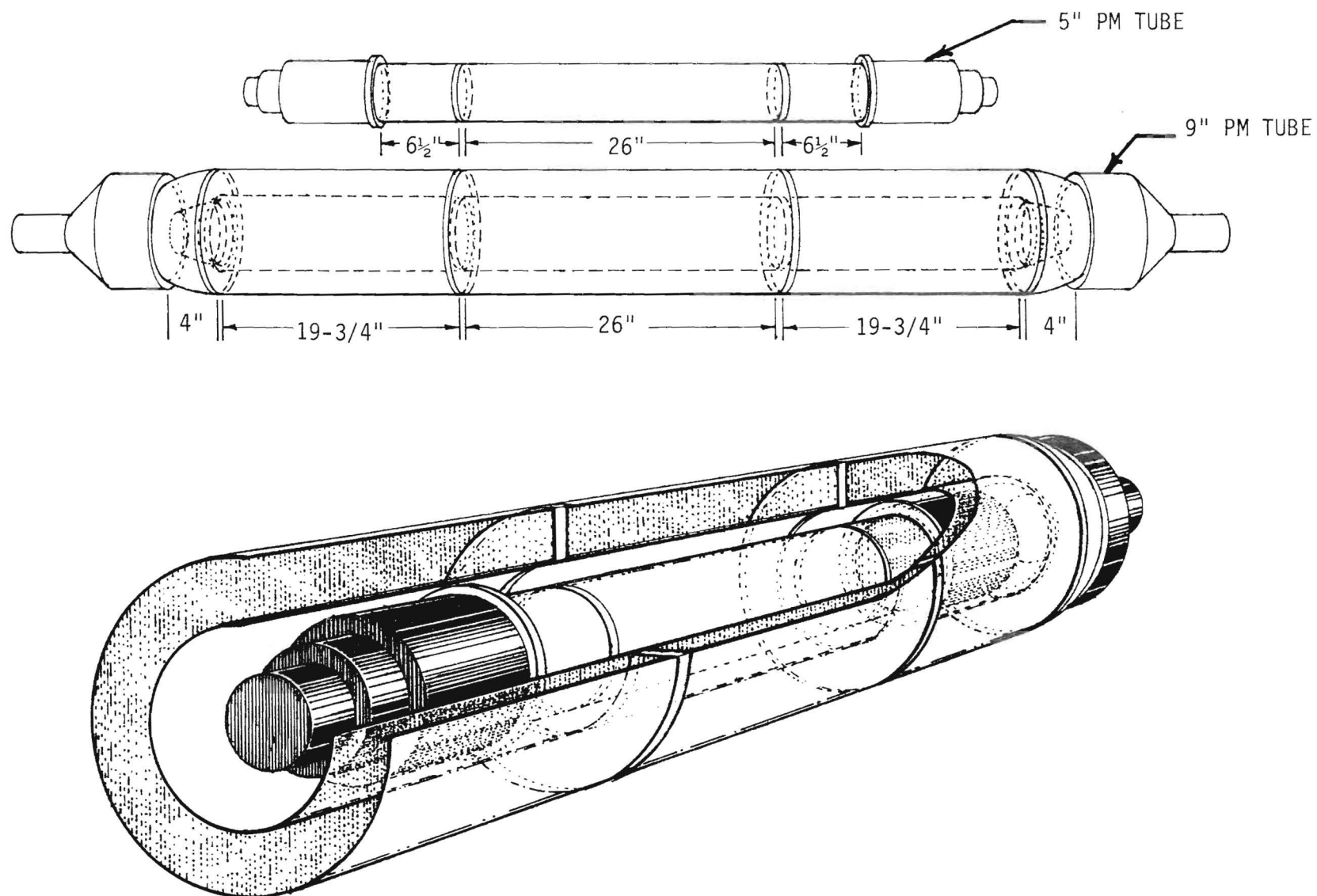
55

FIGURE 23. DETAILS OF THE PROTOTYPE DETECTORS AND MODULE
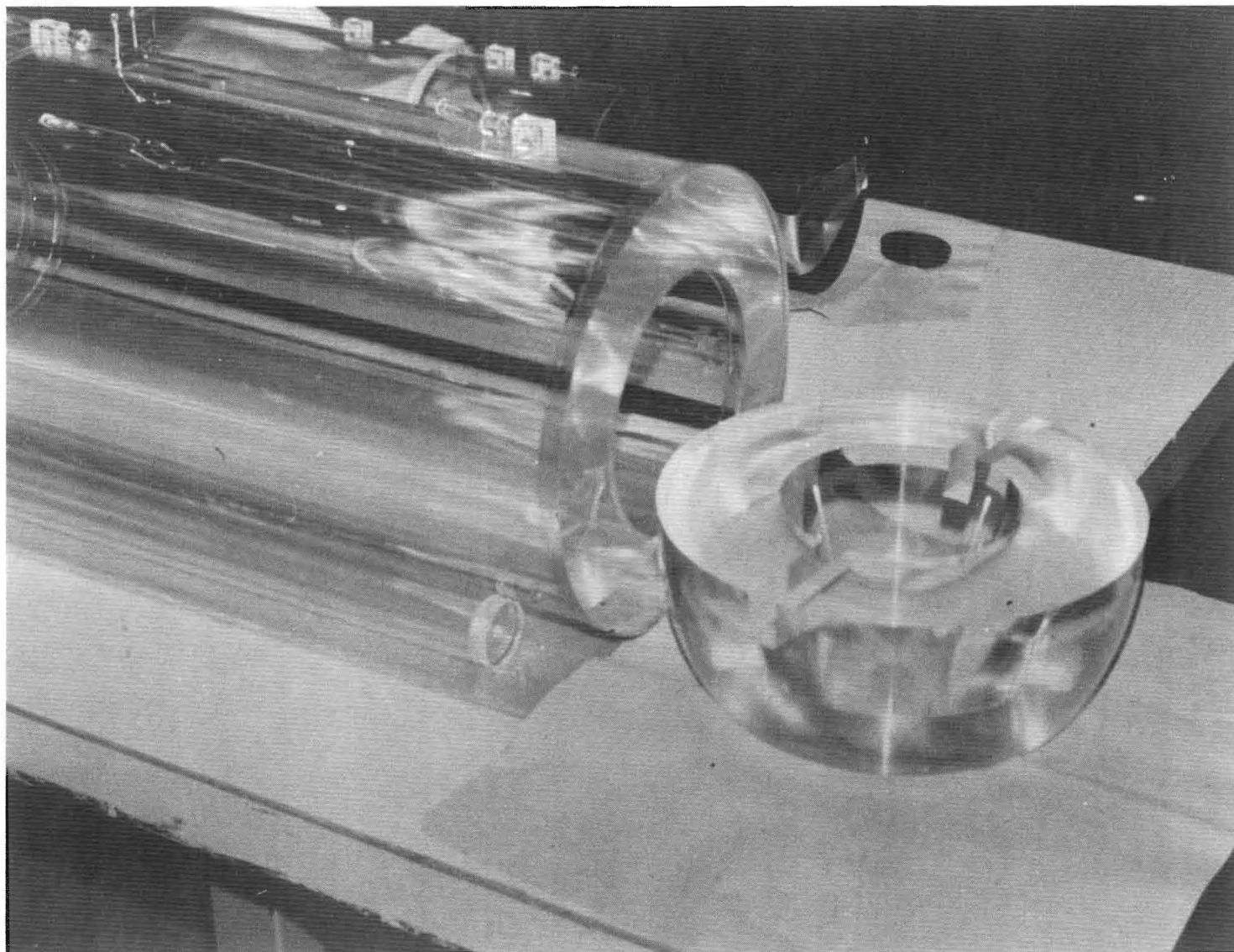
FIGURE 24.   PHOTOGRAPH OF DISASSEMBLED OUTER DETECTOR LIGHT PIPE

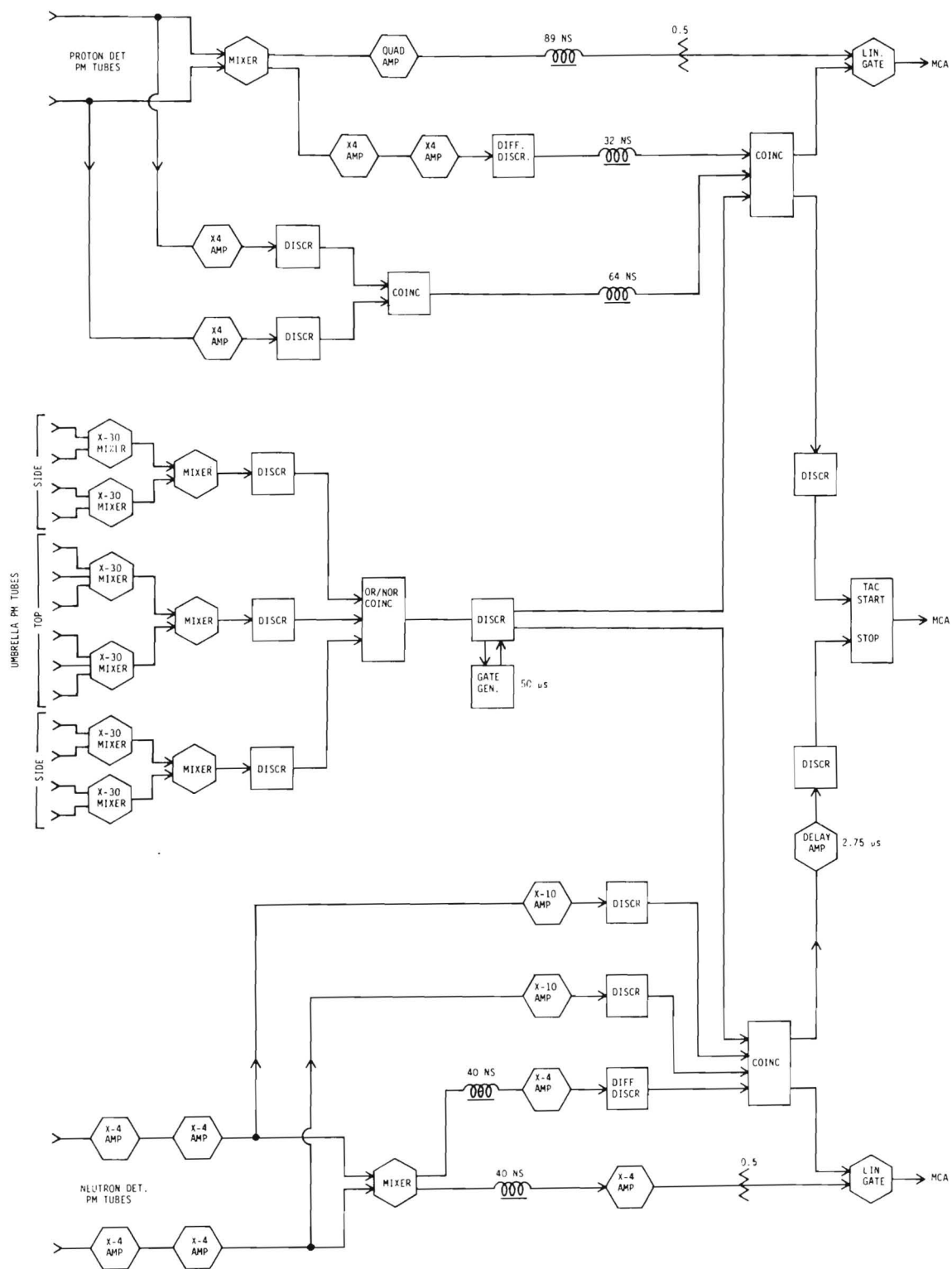FIGURE 25. SCHEMATIC OF PROTOTYPE MODULE EXPERIMENTAL ELECTRONICS

A - WITHOUT PROMPT REJECTION
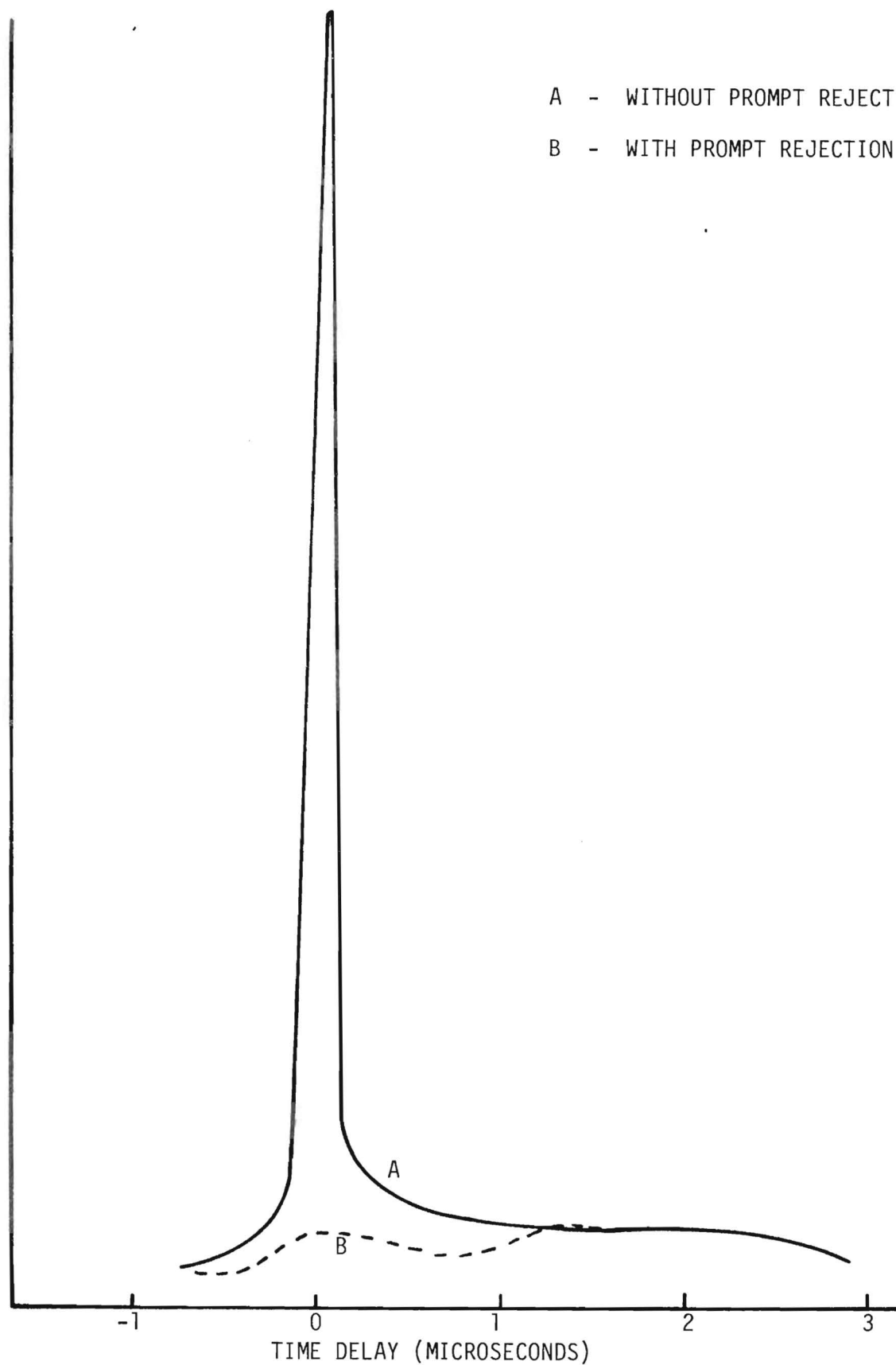
B - WITH PROMPT REJECTION

FIGURE 26.   PROTOTYPE MODULE TIME DELAY SPECTRA

58

The introduction of both a 500 microsecond wide cosmic ray anticoincidence requirement and the prompt rejection requirement allowed the collection of the delay spectrum shown in Figure 27. These rates, corrected for dead time, are quite low. The remaining peak around zero delay appears to be related to the efficiency of the cosmic ray anticoincidence umbrella. Although the umbrella provides good coverage of the central detectors, it does not cover the ends of the bulk shield. Consequently, cosmic ray interactions in the end portions of the shield can cause events in the detectors which are not vetoed by the umbrella. The effects of a more efficient umbrella, as well as other optimization of the system, will be investigated as the study progresses.

The scintillator which is used in the outer detector of the prototype is not the lithium-6 loaded scintillator. The present construction material, plexiglass, would allow degradation of the scintillator over long storage periods. An outer detector constructed of a material such as steel, quartz, or low background glass is needed for the containment of the lithium-6 scintillator. The selection of such a material and the fabrication of an outer detector is necessary before a test of a module containing the lithium-6 is possible. The present prototype is being used to examine several characteristics of the detector system. It allows measurement of the chance signatures under laboratory conditions. It allows an investigation of the time correlation characteristics of the coincidence events. It allows a determination of the radiation environment within the outer detector. The outer detector shields the inner detector from external radiation, and a measurement of this effect will be possible. In fact, for the purposes of this feasibility study, lithium loading is not necessary.

Data Collection And Analysis Scheme

In a low data rate experiment, such as the proposed neutrino experiment, it is essential that the maximum amount of information be recorded for each event detected. This is particularly essential when the recording of accidentals and/or background events would require counting times at least as long as event recording times, in order to obtain statistical significance.

In view of the nature of the signature of the neutrino-induced breakup of the deuteron in the proposed multiregion detector system, and the possible false, background and accidental events, the data collection system for the proposed experiment must be designed to allow for collecting and analyzing a
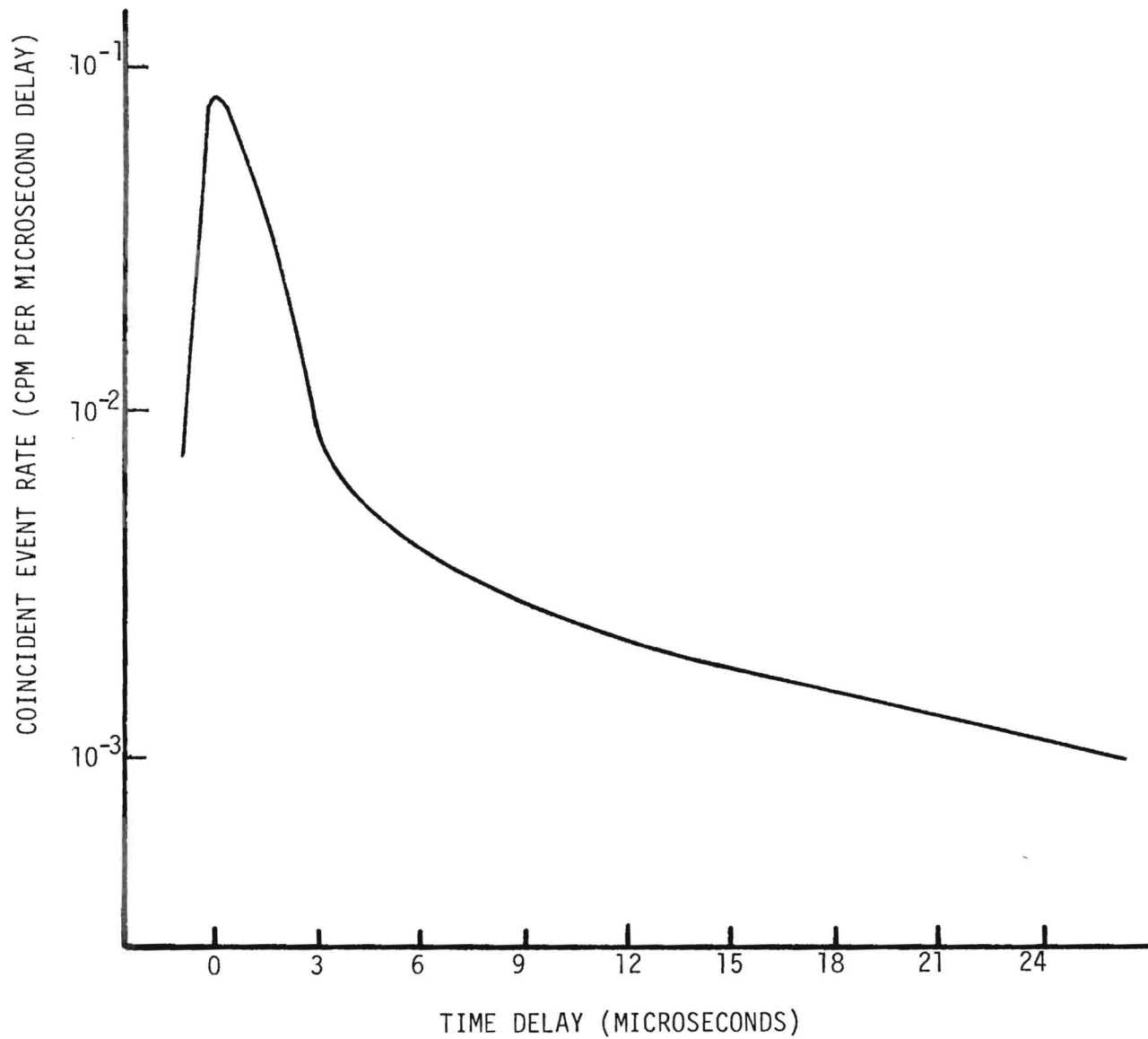
FIGURE 27.   PROTOTYPE MODULE TIME DELAY SPECTRUM

60

wide range of data, for both energy and time correlation, from a group of two-region liquid scintillation detectors. For this type of experiment to be accomplished in a practical time, the maximum information must be recorded during the real counting time.

For each region of the detectors, the energy of each event of interest must be recorded, as well as the delayed time correlation between events in corresponding "proton" and "neutron" concentric detectors. In addition, in a multi-module detector system, information concerning the events occuring in other modules, during or immediately preceeding the delayed coincidence window, can provide valuable data for analysis of background, accidentals, cosmic ray shower induced events, etc. Additional information required for later analysis includes time of day, reactor power level, singles rates in each detector, live (or dead) time of the system, energy calibrations, etc. To obtain the maximum information during the data collection interval, for both "on-line" and subsequent "off-line" analysis, a minicomputer based collection system is proposed. In this system, all data collected will be formatted and stored on computer readable media for later analysis and evaluation. In as much as possible, electronic "thresholds" will be set as low as practical, and energy windows set as wide as practical, so that in the later data analysis, the events may be examined with thresholds and windows set by alternate analysis criteria, rather than having to repeat the data collection for multiple threshold and window settings. This approach is practical with the data collection system planned. These data will be analyzed for those events which meet the theoretical criteria of the neutrino induced breakups of the deuteron in the central detectors. Due to the low expected rate of events, it is essential that a maximum amount of information on each event be retained, so that the data can be examined on an event-by-event basis, subject to the appropriate criteria.

To this end, the hodoscopic data collection and analysis system has been designed to record, for each event fitting minimum criteria in each of the concentric detector modules, the following (as screened by the anticoincidence-event signature logic, see Figure 28):
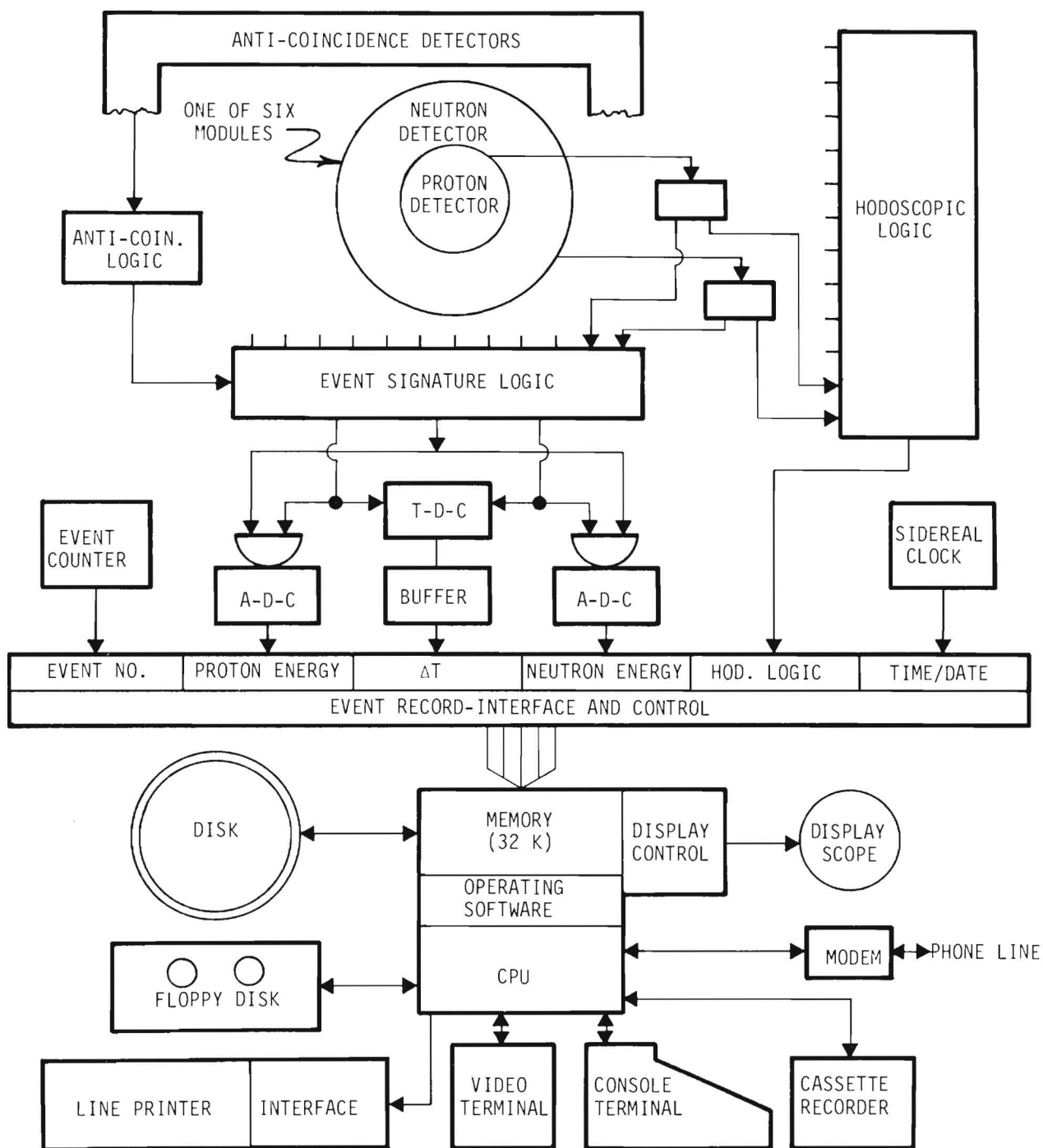
FIGURE 28. DATA COLLECTION AND ANALYSIS SCHEME

1. The pulse height in the proton detector region (i.e., deuterium target).

2. The pulse height of an event occuring within the delayed coincidence window in the neutron detector.

3. The time between events in the two regions.

4. Hodoscopic correlation data concerning events occuring during the delayed coincidence window in other detector modules.

5. Time, data and event number. (Identification for later sorting and analysis and correlation with reactor power level. Sidereal time is preferred here for correlation with cosmic ray activity.)

These raw data will be saved "as is", for later detailed sorting and analysis. By using a general purpose minicomputer for the formatting and data collection, the data on the events can be saved on magnetic storage media for later detailed analysis. In addition, summary information can be generated for on-line experiment analysis, monitoring, calibration and control. While the data collection is the primary task, the low event rate will allow ample time for background tasks, including these on-line monitoring functions. Suitable displays will be generated for the "operator" to allow for rapid evaluation of experiment performance. A specialized interface between the analog-to-digital converters, event detectors, and timers, and the computer must be constructed.

Provision is made for multi-media data recording for reliability and even for remote read out and monitoring over phone lines.

Each detector module, consisting of a deuterated target/proton detector and a concentric lithium-loaded scintillator/neutron detector has associated with it a time-to-digital converter (TDC), and a two-bit status register, in addition to the normal signal conditioning and fast coincidence/anticoincidence electronics.

The TDC is used to determine the interval between "acceptable" events in the proton detector, and subsequent events in the other detectors, within the delayed coincidence window. The length of the delayed coincidence window is determined by the range of the TDC, in that "overflow" of the TDC terminates the delayed coincidence period (about 33 microseconds). Once an "acceptable" event occurs in the central proton detector, the TDC is initiated and counting begins. The condition of the status register bits of all modules is saved in a buffer memory at the same time, indicating which detector (or detectors) fired within the selected prompt coincidence resolving time. During the delayed coincidence window, the occurence of any event in any detector of the system causes the recording of the current elapsed time from the TDC, and the current status bits

63

of all the detectors in the buffer memory. At the end of the delayed coincidence interval, as determined by the TDC overflow, the buffer memory will contain a complete time correlation record of the event, including which detector initiated the event, the delay time at which the corresponding neutron detector fired, and whether any other detector, including the initiating detector, fired during the delayed coincidence window. The status bits of the detectors provide the hodoscopic information on time and space correlated pulses, and on certain "accidentals", and false signals, that might otherwise be masked by the electronics. If no neutron event occurs in the corresponding neutron detector during the delayed coincidence interval, the event is flagged as a false start and the system is reset. The information on such "false" starts is retained for later use in the analysis of background, accidentals, etc.

The use of a time-to-digital converter with buffer memory, rather than a time-to-amplitude converter, permits the detailed recording of the time correlation of the occurrence of any event in any detector after an initiating event is detected, not just the interval to the first event in the corresponding neutron detector. Combined with the hodoscopic information, this will provide a more direct means of evaluating the various events which could occur during the relatively long delayed coincidence period. Although some of these events could be rejected electronically, the nature of the experiment suggests strongly that these events be recorded for later use in analysis and evaluation.

The signature of an antineutrino-induced deuteron disintegration is the occurrence of a pulse in the deuterated target/proton detector region followed by a delayed coincidence pulse in the concentric lithium-loaded/neutron detector region. Both pulses must lie in appropriate energy ranges and be in anticoincidence with the cosmic ray guard detector to be considered an event of interest. To reduce the background from cosmic ray shower fast neutrons and gamma rays, the system provides for a fixed anticoincidence gate time which is sufficiently long (about 750 microseconds) to permit the capture or escape of shower produced neutrons. (This is consistent with studies of such events and their time correlation. C.F. Harold May and L. D. Marinelli, "Cosmic Ray Contribution to the Background of Low-Level Scintillation Spectrometers" (p. 474) in THE NATURAL RADIATION ENVIRONMENT, J. A. S. Adams and W. M. Lowder, eds., William Marsh, Rice University (1964). Also H. S. Gurr, private communication.) This long

dead time, for each guard detector event, requires careful determination of the system "live time" in order to evaluate the "true" event rate. A gated clock will be provided, which will record the elapsed live (or dead) time in a manner similar to that used in conventional pulse height analyzers.

In addition to the TDC data, pulse height data for each detector region is obtained from conventional nuclear analog-to-digital converters (ADC's) which are appropriately coincidence-anticoincidence gated. These are directly inter-faced to the small computer and are read along with the TDC buffer, time, date and event number on detection of the event flag.

Each event recorded then will be in the form of a series of binary words, specifying the various parameters measured. The use of a small computer, with bulk storage, permits the formatting of these data for convenient later analysis, and, in addition, the accumulation of summary data and the presentation of these data for "on-line" monitoring and control by the experiment operator.

The system proposed provides for the storing of raw data on a sequential event-by-event basis, and the concurrent recording and displaying of a wide variety of summary data for the experimenters' evaluation and action. Calibration spectra, selected singles rates and other such data are kept as part of the data file.

When a statistically significant number of events are collected, these data will be screened and analyzed by software determined criteria. By keeping the raw data in machine readable form, they may be analyzed under various alternate criteria, including different energy thresholds, time distributions, etc.

9" Diameter Central Module Prototype

The encouraging results obtained so far support a possible experimental simplification which would apportion the available 40 liters of deuterated octane among two rather than six modules. The simplification occurs in the re-duced number of modules and in the less complex data analysis and collection scheme necessary for two modules. A smaller shield would suffice for two modules. The costs of module fabrication, electronic components, and shielding materials would be reduced.

The increase in size is made practical by the existence of potentially suit-ably fast nine inch diameter photomultiplier tubes. The general features of each module would be similar to those displayed in Figure 23, appropriately

scaled. An eight inch diameter inner detector would match the nearly eight inch diameter active photocathode area. The length of the sensitive volumes of each detector would remain nearly the same. Three nine inch diameter photomultiplier tubes would view each end of the outer detector. The design of an eight inch diameter prototype inner detector is in progress.

Other Investigations

The plan for the ORELA experiment is being coordinated with Dr. S. Raman of Oak Ridge National Laboratory. The scintillation cell for the experiment has been constructed.

The calculations of the gamma ray response of liquid scintillators and the neutron transport properties of the experimental modules are being actively pursued. Data are being collected for the recalculation of the fission antineutrino spectrum.

Section E

PRELIMINARY FEASIBILITY ANALYSIS

The data obtained to date and described in the preceeding sections lead to some positive conclusions about the feasibility of the proposed experiment. All aspects of the experiment design have now been investigated to some degree. Although some of the investigations are not yet complete, the data are adequate to demonstrate feasibility.

The goal of the experiment is not only to detect the existence of the weak neutral current by observation of the low energy electron antineutrino disintegration of the deuteron, but also to obtain an accurate measurement of the cross section. The experiment is designed to define an antineutrino induced deuteron disintegration event signature which is sufficiently restricted to avoid most extraneous events, and to allow accurate measurement of the experimental parameters such as efficiencies, energy thresholds, etc.

In the antineutrino disintegration of the deuteron,

$$\bar{\nu}_e + D \rightarrow p + n + \bar{\nu}_e' \tag{14}$$

the detectable products are a proton and a neutron. The experimental arrangement allows the direct detection of the proton and the measurement of the energy of the proton deposited in the deuterated target scintillator. The neutron is detected after a migration and thermalization time in the concentric lithium-loaded scintillator. The energy recorded from the neutron detector is not that of the neutron, but the energy of the alpha/triton pair produced in the exothermic reaction of the neutron and a ^{6}Li nucleus,

$$n + {}^6Li \rightarrow {}^4He + {}^3H + 4.8 \text{ MeV.} \tag{15}$$

Three experimental parameters are used to delimit the signature of the antineutrino-deuteron reaction. They are:

1. Proton Energy Window $= \Delta E_p = 0.1$ to 1.0 MeV,
2. Neutron Energy Window $= \Delta E_n = 0.30$ to 0.65 MeV (electron equivalent energy),
3. Capture Time Window $= \Delta \tau = 0.1$ to 33 microseconds.

Two additional experimental constraints acting within each module provide for
rejection of unwanted signatures;

1. Prompt Rejection Time Gate $= \pm$ 0 to 100 nanoseconds,
2. Cosmic Ray Anticoincidence Time Gate $=$ 500 microseconds.

Additional module-to-module rejection constraints will be applied in the
final multiple module configuration.

The event rate to be determined from the experiment is that of the reaction
(14). For this experiment, it has the predicted value of 1.8 per hour.

$$I_o = \phi_{\bar{\nu}_e} \, \sigma_{\bar{\nu}d} \, N \; = 1.8 \text{ per hour} = 43.5 \text{ per day}, \qquad (16)$$

where:

$$\phi_{\bar{\nu}_e} = 3 \times 10^{13} \text{ cm}^{-2} \cdot \text{sec}$$

$$\sigma_{\bar{\nu}d} = 6.5 \times 10^{-45} \text{cm}^2$$

$$N = 2.58 \times 10^{27} \text{ deuterons/40 liters}$$

The actual detected rate, S, due to this reaction will be smaller by a
factor determined by the experimental efficiency and the number of reaction
products falling within the signature limits.

$$S = k_p \cdot k_n \cdot k_\tau \cdot I_o = 0.85 \text{ per hour} = 20.4 \text{ per day}, \qquad (17)$$

where the fractions k_p, k_n and k_τ are the fractions of the total number of
$\bar{\nu}e$ events which fall within the signature constraints ΔE_p, ΔE_n and $\Delta \tau$. The
values are:

$$K_p = 0.58$$

$$K_n = 0.90$$

$$K_\tau = 0.90.$$

The measurement consists of a difference between signature event rates with the antineutrino flux present and not present. Adequate shielding isolates the detectors from the other radiations of the reactor and the experimental arrangement allows discrimination against the other antineutrino induced events. (See Section B.) These precautions alone would allow a measurement of the antineutrino induced deuteron disintegration event rate to any desired precision given sufficient time. The restraints imposed by long term instrumentation instability and the resources of the experimenter require that the time to produce the desired result be reasonable. Consequently, a feasibility analysis should emphasize those parameters which affect the counting time.

The counting time was shown in Section B to have the form

$$T = 2B(k/S)^2,$$ (18)

where B is the background rate and k is the constant specifying the statistical accuracy of the measurement. This now reduces to

$$T = 0.0048k^2B \text{ days}$$ (19)

or for k = 4, a reasonable requirement for a statistically significant result,

$$T = 0.076B \text{ days}.$$ (20)

The background signature event rate B can be expressed as the sum

$$B = B_1 + B_2 + B_3,$$ (21)

where B_1 includes all observed correlated events producing the event signature (i.e. from reactions 1a through 1g, Section B, page 8), B_2 all observed correlated events which synthesize the signature, such as the scattering of a gamma ray from one detector to another, and B_3 all observed signatures due to the chance synthesis by uncorrelated events.

69

The rate B_1 consists of the sum of rates due to the neutron, gamma ray, and antineutrino fluxes within the shield. The largest term of this sum is the rate of photodisintegration of the deuteron, for the ratio of neutron to gamma ray fluxes is low.

The rate B_2 also consists of a sum of rates, each due to the scattering of different particles. The neutron portion is negligible compared to the others, and for the same reason of reduced flux. The rejection of correlated scattering events is accomplished by the rejection of signatures which are in prompt coincidence in the two detectors of a module. This eliminates those scattering events caused by swift particles.

The chance rate B_3 consists of a product of the rate of events in each of the two detectors in a module. All sources of events contribute, including electronic noise.

The experimental results obtained so far include measurements of $B_2 + B_3$ for various experimental conditions (See Section D). The rate of photodisintegration events, $I_{\gamma d}$, was calculated (Section C) and the observed rate, the leading term of B_1, was obtained by applying the signature delimiter parameters to the nucleon energy distribution calculated for the photodisintegration process. The values so obtained for B are as follows:

$$B_1 = k_p \cdot k_n \cdot k_\tau \cdot I_{\gamma d} \tag{22}$$

$$= (0.49)\,(0.9)\,(0.9)\,[4.25] = 1.7/\text{hour/module}$$

$$= 10.1/\text{hour/40 liters}$$

$$= 258/\text{day/40 liters}$$

$$B_2 + B_3 = 6.2/\text{hour/module} = 37/\text{hour/40 liters} \tag{23}$$

$$= 888/\text{day/40 liters}$$

$$B = B_1 + B_2 + B_3 = 8/\text{hour/module} = 48/\text{hour/40 liters} \tag{24}$$

$$= 1{,}313/\text{day/40 liters}.$$

70

It is now possible to estimate the counting time, T, for the proposed experiment. Substituting the background rate, B, from equation (24) into equation (19) gives,

$$T = 5.43k^2 \text{ days} \tag{25}$$

or from equation (20)

$$T = 76 \text{ days.} \tag{26}$$

There is good justification for viewing this computed value of the counting time as an upper limit to that which will actually be achieved. Several important effects were not included in the data and each can only reduce the value of T. These effects are:

1. Application of prompt rejection for module-to-module scattering. At present the only prompt rejection is that between detectors in a single module.

2. Incomplete coverage of the bulk shield by the present cosmic ray umbrella detectors.

3. Incorporation of the planned data collection and analysis instrumentation will allow exact optimization of the values for the event signature delimiters. This is not possible with the present instrumentation.

4. Greatly increased overburden at the experiment site compared to the negligible amount at the present site.

It is not unusual for neutrino experiments to consume many months or even years of counting time. The fundamental limitation on the length of counting time is the requirement of maintaining apparatus and instrumentation calibration so that accumulated data may be legitimately integrated. Very careful and detailed consideration has gone into the development of instrumentation and procedures for calibrating and monitoring performance. All of which produce a "coherence" time certainly measured in years. Thus not only is the proposed experiment feasible, but a very high degree of statistical accuracy is probable.